ISLAMIC UNIVERSITY OF TECHNOLOGY

ORGANISATION OF ISLAMIC COOPERATION

Optimized Design of an Off-Grid PTC Based Power Plant in Saint Martin's Island

B.Sc. in Mechanical Engineering Thesis

Authors

Md. Khairuzzaman

Student ID: 160011003

Md. Raihanul Islam

Student ID: 160011041

S.M. Maheer Asef

Student ID: 160011072

Department of Mechanical and Production Engineering (MPE)

Islamic University of Technology (IUT)

March 2021

ISLAMIC UNIVERSITY OF TECHNOLOGY

ORGANISATION OF ISLAMIC COOPERATION

Optimized Design of an Off-Grid PTC Based Power Plant in Saint Martin's Island

A THESIS PRESENTED TO THE DEPARTMENT OF MECHANICAL AND PRODUCTION ENGINEERING, ISLAMIC UNIVERSITY OF TECHNOLOGY IN PARTIAL FULFILMENT OF THE REQUIREMENT FOR THE AWARD OF THE DEGREE

BACHELOR OF SCIENCE (B. Sc.) IN MECHANICAL ENGINEERING

Authors

Md. Khairuzzaman

Student ID: 160011003

Md. Raihanul Islam

Student ID: 160011041

S.M. Maheer Asef

Student ID: 160011072

Supervisor: Dr. Md. Rezwanul Karim, Assistant Professor

Department of Mechanical and Production Engineering (MPE)

Islamic University of Technology (IUT)

March 2021

Certificate of Research

The thesis titled "Optimized Design of an Off-Grid PTC Based Power Plant in Saint Martin's Island" submitted by Md. Khairuzzaman (160011003), Md. Raihanul Islam (160011041) and S.M. Maheer Asef (16001172) has been accepted as satisfactory in partial fulfillment of the requirement for the Degree of Bachelor of Science (B.Sc.) in Mechanical Engineering.

Thesis Supervisor

Dr. Md. Rezwanul Karim

Assistant Professor

Department of Mechanical and Production Engineering (MPE)

Islamic University of Technology (IUT)

Gazipur, Bangladesh

Candidates' Declaration

It is hereby declared that, this thesis or any part of it has not been submitted elsewhere for the award of any degree or diploma.

Signature of the Candidates

Md. Khairuzzaman
Student ID: 160011003

Md. Raihanul Islam
Student ID:160011041

S.M. Maheer Asef
Student ID: 160011072

Department of Mechanical and Production Engineering (MPE)
Islamic University of Technology (IUT)
Gazipur, Bangladesh

Acknowledgment

We would like to begin by saying Alhamdulillah and grateful to Almighty Allah who made it possible for us to finish this work successfully on time. We also want to thank our supervisor Dr. Md. Rezwanul Karim, Assistant Professor, Department of Mechanical and Production Engineering, IUT for all his support, time, ideas about the problem, explaining patiently the hard topics and checking this thesis and papers above all his care and concern. These will ever remain in our memory. Thanks to our examiners for their constructive ideas, suggestions and double checking our work.

Contents

List of Tables

List of Figures

Abstract

Solar energy is one of the key renewable energy sources of the globe and can be converted into power by using different technologies and approaching various methodologies. As a remote island and being disconnected from the national power grid, Saint Martin's island in Bangladesh is one of the best prospects for mass scale usage of solar power. Solar energy can be converted to electrical power by two distinct processes namely Photovoltaic (PV) conversion and Concentrating Solar Power (CSP) using thermodynamic cycles. Concentrating Solar Power (CSP) is thought of as one of the major future alternatives in the field of harvesting solar energy. It has advantages over the PV cells in terms of efficiency and lifetime. Using thermal storage technology integrated with the CSP plant, about 6 to 12 hours of power backup can be gained in ideal conditions. In this study, a 1 MW parabolic trough collector (PTC) based stand-alone CSP power plant with 12 hours of thermal storage has been specifically designed and optimized for Saint Martin's island using System Advisor Model (SAM). The design point DNI value selected for the specified location is 852 W/m$^{2.}$ The gross power cycle output for the optimized plant is calculated to be 2.68 GWh with a power cycle efficiency 40.58%. The total land area needed for the proposed design plant is 7.83 acres which covers only 1.08% of the total land area of this island. The proposed design of the PTC based thermal power plant resolves the power generation problem of a disconnected island of the country which will in turn develop the daily life of locals along with making the travelling experience smoother for the tourists. The performance analysis of the plant also encourages development and innovation of solar thermal power plants in Bangladesh.

1. Introduction

The indication of a society's development is often being measured through the development of energy production and consumption of that society. Energy is an essential tool for the substantial development of a prospering society. The main reason behind that factor is home appliances, industries, automobiles even agricultural production has now become quite dependent on the consumption of energy. So, with ever growing advancement of all the aspects of life, the dependency on energy is becoming more relevant than ever before. Keeping that in mind, we are bound to use a heavy amount of fossil fuel to produce and meet these large energy demands which in turns plays a vital role in greenhouse effect and the overall emission of CO_2 gas worldwide. Thus, the solution to these ever-growing energy demand dealing with the environmental effect is only by shifting more towards Renewable energy.

For a growing country like Bangladesh the challenge to meet the energy demand especially electrical energy demands is quite significant. It is very important as well as challenging to meet and fulfil the energy demands of the country for its development in terms of sustainability. Whereas, the total energy demand throughout the world is expected to rise up to 33% by 2030.[1]

At present, major portion of electricity in Bangladesh is being generated by burning coal, fossil fuel, natural gas etc. These all are non-renewable energy. The prime source of energy in Bangladesh is natural gas (about 51%), although the reservoir of natural gas is likely to be depleted by the year 2020.

Currently, the power generation capacity of Bangladesh is more than 21,000 MW and it's rising continuously. But non-renewable sources of energy are not sufficient to meet the energy demand which also growing day by day. It has negative impact on environment also. However, Bangladesh can meet the required energy demand which may ensure the availability of electricity by incorporating potential renewable energy sources like wind, solar, biogas and biomass, lighting, sea-wave, geothermal, and hydro. Currently, the total on-grid energy production from the renewable source is less than 2% (solar, wind, hydro) but the potential of energy from renewable source is huge. If properly harnessed, the energy security for the future development may also be ensured.

Solar energy is one of the most promising ways of going forward with the high demand of the countries' electrical need. For long, solar energy is being used as nuclear energy source in distinct rural areas or even in harvesting crops in some minor areas of the country. But if the proper technique can be applied and the most out of the available solar energy can be used, we can reach to a certain height of sustainable energy supply system for the mass.

The most common technology associated with solar energy in the country is the stand-alone PV home systems to meet basic electricity demand of remote inhabitants. The first grid connected solar power plant of capacity 3 MW has recently been introduced in the country and started to supply power in the national grid from 3rd August, 2017 [2] followed by several other projects. The current total on-grid installed capacity of Solar PV based power is about 142 MW and total (on-grid/off-grid) capacity is about 488 MW [2]. However, there is no presence of Concentrating Solar Power (CSP) using thermodynamic cycles. Although, the opportunities regarding solar power production using CSP technology is quite huge in our country.

Bangladesh receives an average annual Direct Normal Irradiance (DNI) at 1900 $\mathrm{kWh/m^2}$. The area required to generate 100 MW of electricity is about $2\mathrm{km^2}$ with an average DNI of 2000 $\mathrm{kWh/m^2}$[3]. Electricity is being generated in neighboring country India using the similar technology. In Bangladesh, there are some places that receives the required amount of solar irradiance for running a solar thermal power plant [4].

The present work is based on the detailed design approach of a PTC based power plant in Saint Martin's island- emphasizing on the effects of various parameters of the solar block on the performance of the power plant. Saint Martin's island is the only coral island of the country which does not have any connection with national power grid.

Using System Advisor Model (SAM) as the simulating tool, the optimized design of the power plant is studied which is capable to produce a net output of about 1MW. This is more than enough to meet the nearest future demand along with present power demand for this particular place. A detailed modeling and analysis of the power output profile along with necessary results and discussions are being presented in this work.

A detailed design approach of a CSP based standalone power plant using Parabolic Trough Collector is being shown in the work. All the design point parameters are being calculated using the simulating tool. Thermal storage technology has been considered to mitigate the power backup problem. The thermal storage capability of the Heat Transfer Fluid is also being analyzed.

Therefore, the complete project is targeted to solve the power generation problem of an off-grid island using renewable source of energy. The major factors that were considered while designing the plant was:

1. Estimated load demand during the whole year
2. Land mass needed for the power plant
3. Selection of proper methodology
4. Thermal storage for the plant
5. Financial feasibility

The detailed approach towards achieving the desired optimized design is illustrated in the work. This will help to resolve the power generation and storage problem of a remote island disconnected from the central power supply system of a country in a sustainable way.

2. Background of the study

2.1. Saint Martin’s Island Location

St. Martin's Island is the only coral island of Bangladesh located in the northeastern part of the Bay of Bengal, about 9 km south of the tip of the Cox's Bazar-Teknaf peninsula. It forms the southernmost part of the country. Total area of this island is about $3\ \mathrm{km}^2$. A small adjoining island called Chera Dwip, is separated at high tide. It is about 8 kilometers (5 miles) west of the northwest coast of Myanmar, at the mouth of the Naf River.

Geographical location of the site is:
Latitude**:**20°37'22.86"N
Longitude**:** 92° 19' 12.76" E [5]

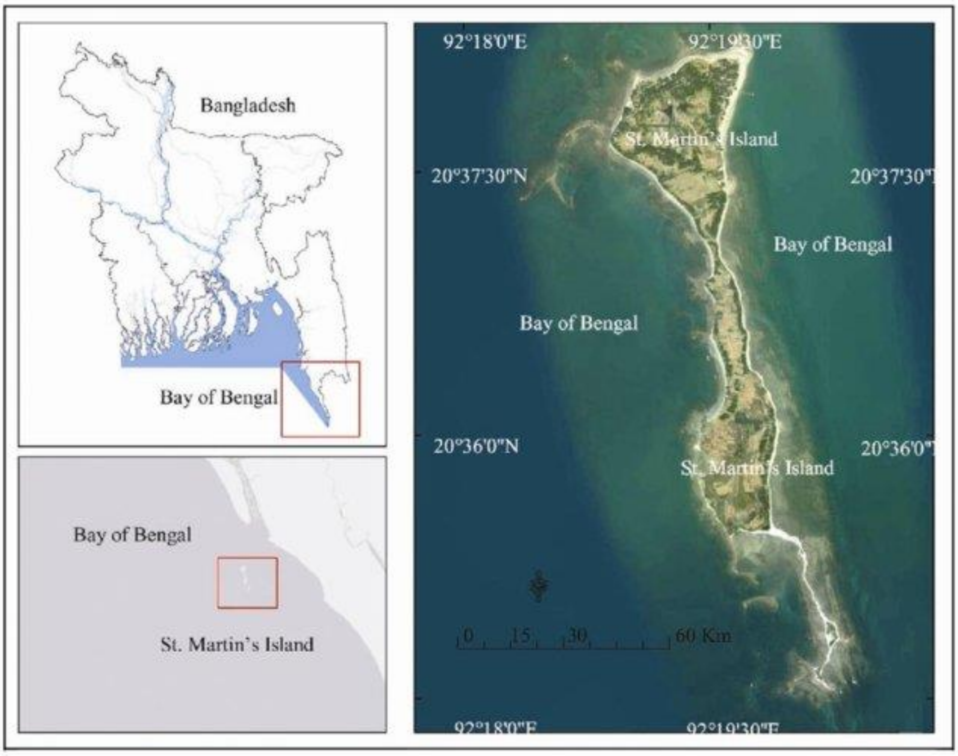

Figure 1: The map of St. Martin's Island, Bay of Bengal, Bangladesh [6]

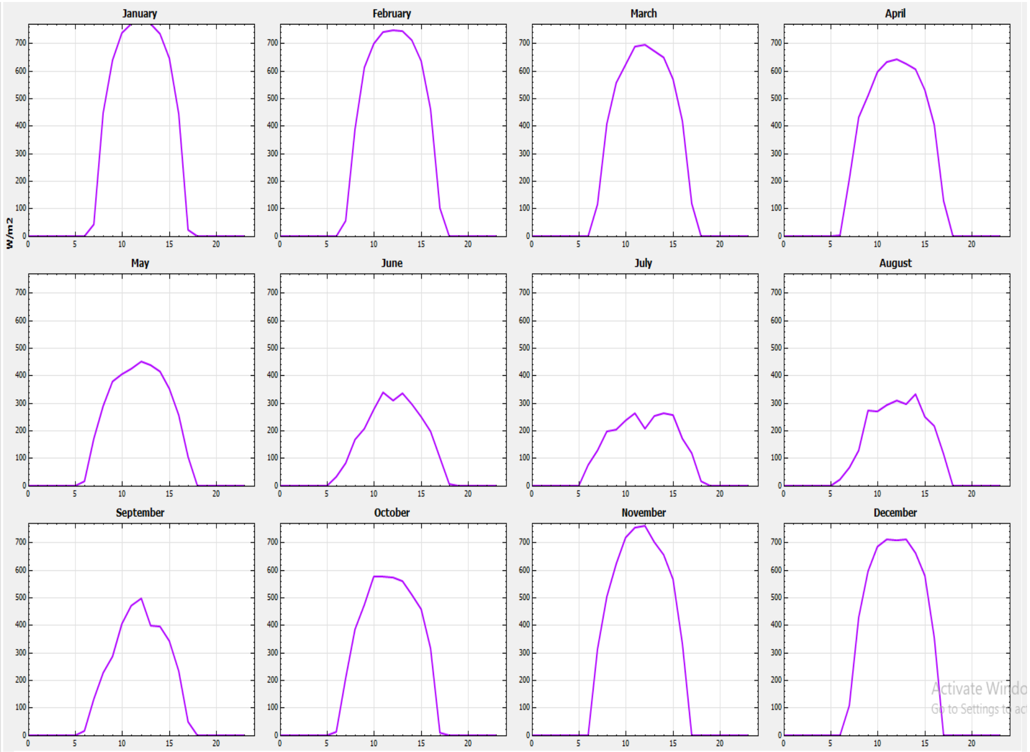

Figure 2: Monthly average DNI of Saint Martin’s island [7]

From the average monthly Direct Normal Irradiance (DNI) values of Saint Martin’s island it is clearly evident that the DNI value differs from month to month. During the months of April to August the duration of daily solar irradiance lasts for a significant amount of greater time. Whereas, during winter (between November to February) the DNI values are not being spread throughout a longer period of the day rather it reaches a peak value during midday then again gets lowered within a short period of time.

2.2. Saint Martin as a Tourist Destination

As the only coral island of the country, Saint Martin’s Island is one of the major eco-friendly tourist destinations of the whole country. The mesmerizing beauty of the blue ocean along with the hilly view from the other side of the ocean makes it more compelling for the tourists. Due to limited land mass and restrictions imposed by the government on multi storied buildings, most of the resorts and hotels are located near the beach. The astounding sound of waves hitting the shore along with glazing moonlight enhances the beautification to an unimaginable limit. Also, some homestay facilities are often being found during hazardous conditions. Altogether there are about 34 registered local tourist guides to serve the need of the tourists.

There is an estimated 480-500 persons directly involved with the tourism business along with an additional similar amount of people indirectly involved with it, making a total of about 800-1000 persons' involvement in the tourism business. These directly or indirectly involved personas maintain their families of about 4-6 persons making the possible feeding of about 4800 local residents [6]. Therefore, it can easily be said that, tourism is the prime business of the island contributing not only towards the economic betterment of the locals but also makes the travelling experience of an individual smoother and more compelling.

Figure 3: Saint Martin's Island

2.3. Existing Power Systems of the Island

2.3.1. Small Scale Diesel Generators

Most of the commercial tourist resorts and hotels use small scale generators for meeting individual small scale power demand. These generators are usually operated by using diesel as the fuel.

Figure 4: Small Scale Diesel Generator

2.3.2. Solar Photovoltaic (PV) Arrays

Besides using small scale diesel generators many of the local residents and also some of the resorts and hotels use Solar PV arrays as individual power sources. The power output of these solar arrays is not capable enough to meet the power demand. Also, as there is no option kept for power storage by using this technology, backup power is not possible with this setup resulting in almost negligible power outputs after sunset.

Figure 5: Solar PV Array

2.3.3. PV Based Private Power Plant

Recently, there has been a development of a private PV based power plant in the location. The capacity of the power plant is listed below:

Table 1: Existing power plant specifications

Number of panels	900
Power output per panel	270 W
Total power output	0.243 MW
Produced voltage	150 KV
Backup power source	150 KV Diesel Generator
Per unit (kWh) energy selling price (residential)	32 Taka
Open Circuit Voltage	38.17 V
Max power voltage	31.13 V
Short circuit current	9.18 A
Max power current	8.67 A

The generator used for backup power is filter less. Columns installed for power transmission are 65 feet in height. An initial setup cost of BDT. 5000 is needed while taking connection from the plant merging with another self-centered cost of BDT. 1000.

Figure 6: Currently operational PV plant in St. Martin’s Island

3. Literature Review

3.1. Concentrated Solar Power Technologies

3.1.1. Parabolic Trough Collectors

A parabolic trough solar thermal collector has one straight dimension along with two parabolic shaped dimensions with metal polished mirrors as reflectors. There is a tube through the middle of the collector inside which the heat transfer fluid (HTF) receives solar heat. Mainly, the heated HTF exchanges heat with water and then produces high velocity steam. The produced steam then makes the turbine rotors rotate resulting in the rotation of the central shaft of the generator and hence producing power.

Design cycle efficiency of PTC based power plants usually gets slightly higher than 38% with wet cooling used. Whereas the design cycle efficiency for dry cooled parabolic trough collectors gets (1 to 2) percentage lower than wet cooling [8].

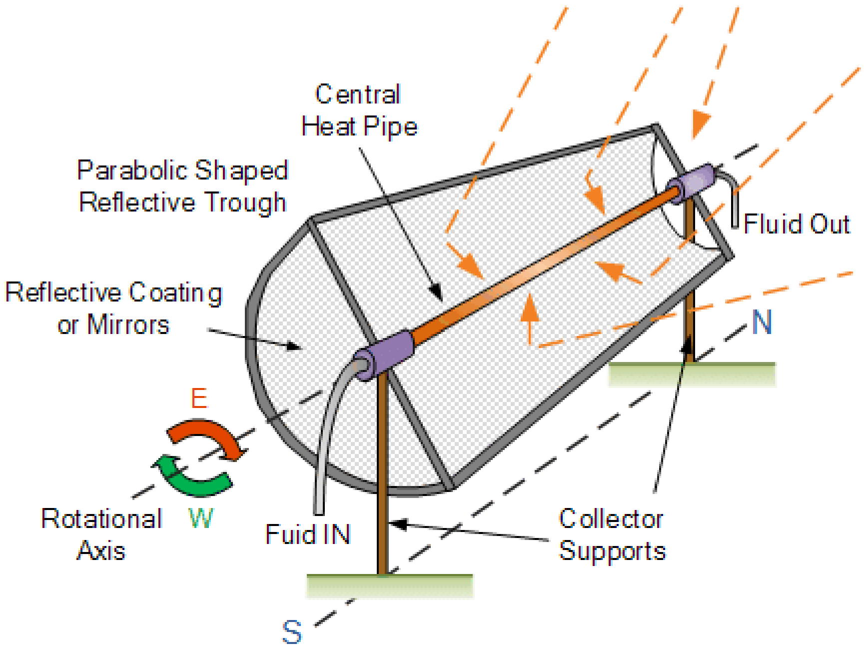

Figure 7: Parabolic Trough Collector [9]

3.1.2. Linear Fresnel Collectors

A series of lengthy thin shallow curvatures (sometimes even flat) mirrors are used to focus incident solar radiation onto one or multiple linear absorbers placed over the mirrors. This technology is particularly designed to reduce the overall plant cost as the wind loads doesn't affect the aperture of heat absorbing element. Also, low grade flat glasses can be used effectively by elastic curving due to the enormous size of curvature of radius of the facets. As the absorber is flat thus the annual output is being reduced compared to parabolic trough collectors.

Usually LFC are used for direct generation of steam at about 55 bar (Novatec Solar PE-2 with 30 MW [10], Liddell steam augmentation system with 9.3 MWth [11]) or superheated steam at moderate temperatures (AREVA Solar's Kimberlina plant at 7.8 MWth [12])

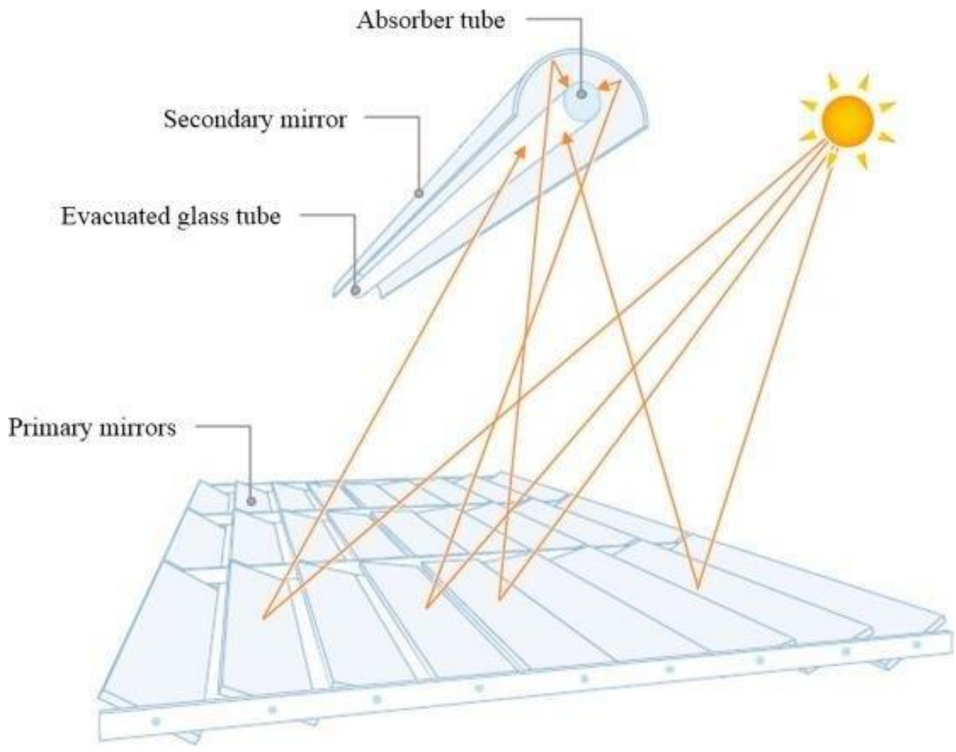

Figure 8: Linear Fresnel Collector [11]

3.1.3. Solar Power Tower

Power towers usually consists of a greater number of heliostats. A heliostat is basically a two-axis tracking mirror with a 20 to 200 m^2 surface. A central tower holds the heat exchanger on the top of it. Solar power tower is best suited for mid-term cost reduction of power compared to PTC. The main reason of it is their ability to further increase the cycle efficiency of gas turbines at above 1000 degrees.

The first commercial solar tower system was commissioned by Abengoa Solar in 2007 which was the Plant PS10 [13]. Terrosol energy erected the solar power tower Gemasolar having a power output of about 19.9 MW_{el} [14][15]. During operation molten salt from cold storage tank flows at about 290℃ to the receiver where the temperature is nearly 565℃. At the steam generator steam of about 540℃ produces power. The heliostat field has 2650 heliostats having a 115 m^2 area of each. The 115m lengthy solar tower has a 15h thermal storage capacity with 24h operating time during summer with an annual capacity factor of 75%.

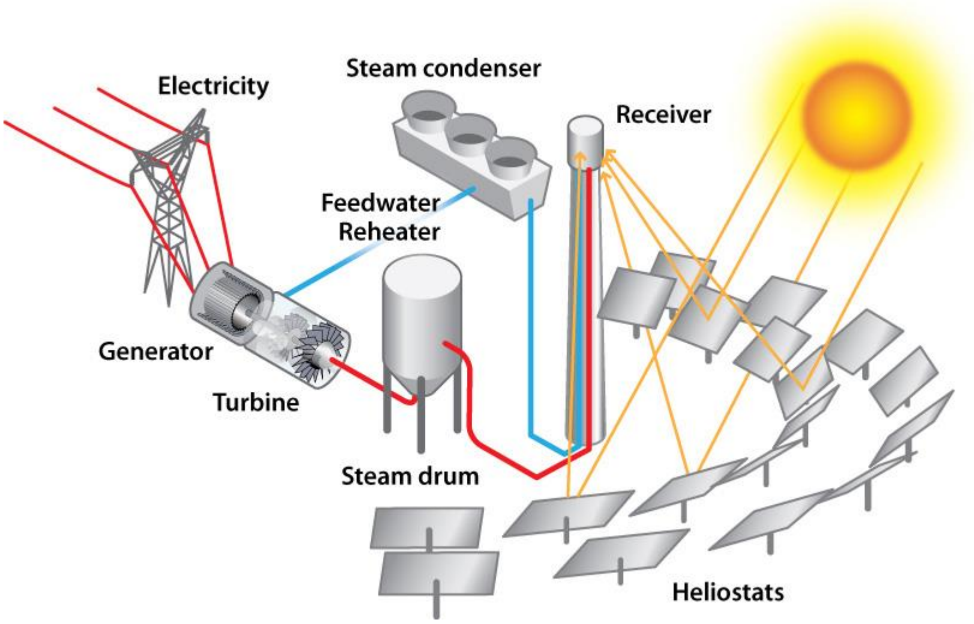

Figure 9: Solar Power Tower [16]

3.1.4. Parabolic Dish-Engine Systems

The main parts of a dish engine system consist of a solar concentrator and a power conversion unit. The concentrator approximates a 3D paraboloid which tracks the incident solar rays. In the thermal receiver concentrated solar beam is absorbed which in turns converts and transfers heat to power production blocks. Stirling engines are the most common type of engine used in Parabolic Dish Engine Systems. Mostly, solar dish engines are targeted towards emerging global markets for distributed generation, green energy, remote power and on grid applications. Commonly individual units can produce power ranging from 9-25 kW. Dish Stirling systems have the lowest share in global CSP market as least as 1% only.

Figure 10: Two units of the 10 kWel EnviroDish installed at the Plataforma Solar de Almeria, Spain. DLR [15]

3.1.5. Comparison of different CSP technologies

Comparison of different CSP technologies in terms of performance data is presented in the Table 2 and Table 3 presented below.

Table 2:Performance Data of Various CSP Technologies [16]

	Capacity/ MWe	Concentration	Peak System Efficiency	Annual System Efficiency	Thermal Cycle Efficiency	Land Use/m^2 $(\mathrm{MW.h.a^{-1}})$
Trough	10-200	70-100	21 %	(10-16) %	(35-42) % ST	6-11
Fresnel	10-200	25-100	20%	(9-13) %	(30-42) % ST	4-9
Power Tower	10-200	300-1000	23 %	(8-23) %	(30-45) % ST	8-20
Dish-Stirling	0.01-0.4	1000-3000	29 %	(16-28) %	(30-40) %	8-12

Table 3: Expected Cost Reduction (of the Components or LEC) or Plant Efficiency Improvement Associated with Technology Innovations [17][18]. Data from ref [18] except if specified.

Subsystems Technology	**Concentrating System**	**Solar Receiver**	**Storage and Heat Exchangers**
Parabolic Troughs[17]	• Mirror reflectivity (93 % today) and new materials: 25 % cost reduction by 2020 • Size and accuracy: 7.5 % cost reduction by 2012, 13 % by 2020 • Support structure:12 % by 2015, 33 % by 2025	•Thermal performance (mainly optical): 14 % efficiency • Glass-metal seal: (2-5) % cost reduction •Higher operating temperature: molten salt, 20 % cost reduction (including effect on storage), 16 % efficiency • DSG: 5 % cost reduction, 17 % efficiency	• Heat exchanger: 10 % cost reduction • Steam generator: 15 % cost reduction • New materials and design: reduction (16-18) % of LEC [18]

Linear Fresnel Systems[19]	• Mirrors and mirror assembly: 17 % cost reduction • Support structure: 10 % cost reduction by 2015	•Thermal performances (mainly optical) •Higher operating temperatures: 117 % efficiency (increase from 270C to 500C)	•Storage development for direct steam generation
Solar Power Towers[19]	•Thin glass mirrors: (1-4) % LEC reduction [18] •Heliostat size optimization: (7-16) % cost reduction • Field optimization: cost reduction 10 %, efficiency 13 % •Tracking system: cost reduction 40% •Support structure design	• Tower (multi-tower): 25 % cost reduction, 15 % efficiency •Higher operating temperature: (40-60) % efficiency increase	•Thermocline tank (molten salt): (25-30) % cost reduction, 1 % LEC reduction [20] •Advanced storage (DSG): (5-7.5) % LEC reduction[18]
Parabolic Dishes[19]	• Concentrator: (43-47) % LEC reduction	• Receiver design for reducing losses and increasing lifetime: (39-40) % LEC reduction	• Stirling engine: (41-45) % LEC reduction • Brayton cycle: (44-51) % LEC reduction

3.2. Previous Works on Solar Power in Bangladesh

There has been a number of research works from authors who have tried to address the issue of solar power in Bangladesh and proposed some solution in small scale. Noor [21] et al. worked on the prospect of concentrating solar power in Bangladesh. It was illustrated that, with an average annual Direct Normal Irradiance (DNI) of 2,000 kWh/m^2 the area required to generate 100MWe of electricity is about 2km^2. The DNI received in Bangladesh is nearly $1900\ \mathrm{kWh/m^2}$ [21]. This amount of solar irradiance is capable to operate CSP based power plants. CSP is already included in the Renewable Energy Policy 2009 by the government of Bangladesh [22].

A 100 kW solar PV based mini-grid started operation in Swandip island, Chattogram from 2010 [23]. Initial investment for this project was $738,267 consisting a 40 kW diesel generator to provide power output through lower radiation period[24].

K.A. Khan [25] et al. worked on the prospect of renewable energy with respect to energy reserve of Bangladesh. Whereas solar photovoltaic technology is best suited to use for [26][27][28]:

- Solar home system (SHS)
- Rural market electrification
- School electrification
- Health clinic/hospital electrification
- Cyclone shelter electrification
- Micro enterprise
- ICT Training center electrification
- Mobile phone charging

Bhuiyan [4] et al. worked on the case study in Bangladesh regarding performance optimization of a CSP based plant located in Cox's Bazaar. A comparative study was carried out on two configurations of a 50MW power plant based on thermal oil and solar salt. The results show that the molten salt-based power plant has higher efficiency (33.19%) than the molten salt-based configuration (31.53%).

The analysis from Bhuiyan et al. [4] is presented in Table 4 where the output parameters of the optimized plants in different locations are tabulated.

Table 4:The viability analysis of the optimized plant for condition of Bangladesh[4]

Parameters	Cox's Bazar (21.43 ° N,91.97°E)	Chittagong (22.27°N, 91.82 °E)	Dhaka (23.77°N, 90.38 °E)	Pabna (24.13°N, 89.05 °E)	Khulna (23.18°N, 89.17 °E)	Rangpur (25.73°N, 89.23 °E)	Sylhet (24.9°N, 91.88 °E)	Rajshahi (24.85°N, 89.37 °E)
Gross-to-net conversion (%)	91.9	91.1	89.6	89.9	88.5	89	89	90.1
Capacity factor (%)	39.5	38.5	32.6	32.4	30.3	30.1	27.2	32.4
Annual energy generation (GWh)	171.08	166.75	141.41	140.65	131.44	130.54	117.98	140.28
Annual water usage (m3)	47,061	46,855	45,148	45,003	44,503	44,278	43,275	44,974
Nominal LCOE (cents/kWh)	9.86	10.I	10.82	11.88	12.68	12.76	14.07	11.91
Natural gas uses (Millions-m^3)	4,845	4722	4005	3983	3722	3697	3341	3973
C02 emission (Millions- m3)	59.88	56.36	49.49	49.23	44.00	45.69	41.29	49.10

Deb [29] et al. worked on the prospect of solar energy in Bangladesh using HOMER as the simulation tool. An off-grid PV based model with storage system was simulated to solve irrigation problems in rural areas. Although the price of the proposed system is higher than grid electricity, this system is capable of providing energy security for 25 years. A thorough discussion on different configurations of solar cooking system along with the potential of the system in Bangladesh was also presented.

3.3. Previous Works on power production and storage in Saint Martin's Island

Some researchers have tried to address the problem of the Saint Martin's Island and presented different idea and method for solving the power problem. These are summarized in the following section.

Karim [30] et al. proposed a 1.3 MW hybrid power plant for saint martin's island. The model specification for the plant is PV (600KW), Wind (200KW), Biogas Generator (250KW),Diesel Generator (250KW) and no of Battery 800 and Inverter (350KW)[30]. The hybrid model configuration is shown below:

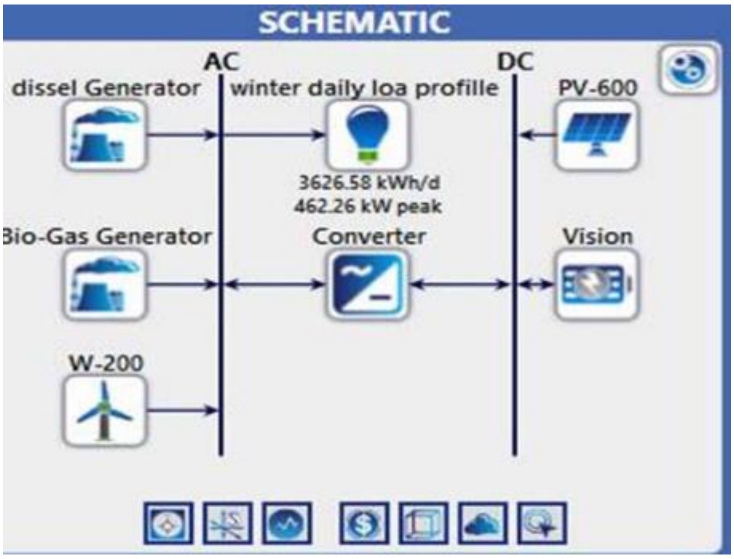

Figure 11:Schematic of the proposed Hybrid power plant [30]

From HOMER output it was presented that,

Net operation cost = BDT 405,024,500.00

Operating cost = BDT 30,668,260.00

Per unit (kWh) cost = BDT 23.67 [30]

Haque [31] et al. worked on an optimized stand-alone green hybrid grid system for Saint martin's island using HOMER. The simulation software synthesized the monthly value of solar radiation using Graham algorithm [32]. The generic cost for a 1 kW plant is considered with a capital cost of $800 [33].

By using wind turbine in the hybrid power plant setup COE percentage increases by 1.13% [31]. With the integrated usage of diesel generators alongside the hybrid system COE reduction is $0.253 from $0.266 [34].

Roy [34] et al. also worked on the hybrid power supply system for Saint Martin's island using HOMER software as well. The results show that with the combination of a PV (85kW), Diesel generator (105 kW), converter (96 kW) and 615 units of batteries is the most commercially viable option for the hybrid system with a least cost of energy is about BDT 19.48 per kWh or $ 0.253 per kWh with total net present cost $ 624,391 or BDT 48,078,107.00 [34].

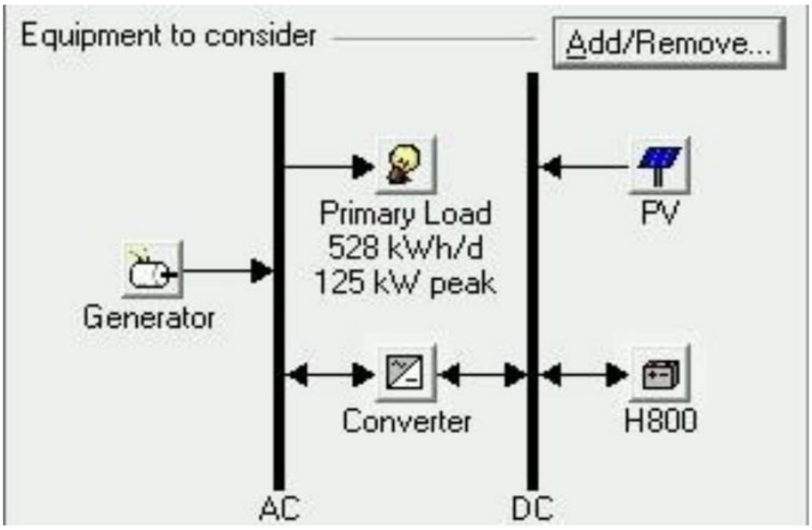

Figure 12 : Complete Model of Hybrid System [34]

The payback period for the hybrid plant is estimated to be 9 years as found from several literatures [35][36].

Mousumi [37] et al. worked on the evaluation of the techno economic analysis of a hybrid power plant in Saint martin's island. the hybrid solar PV/WT system along with backup supply is a realistic solution which includes the initial cost of $ 89,620, the replacement cost of $ 59,791, operating cost of $ 22,701/year, TNPC of $ 250,919 and electricity generation cost of $ 0.206 /kWh [37].

Fardun [38] et al. modeled and optimized a hybrid power plant for coastal area of Bangladesh. Total power output from generator is about 202.631kWh/yr and consumption by DC primary load is about 76,282 kWh/yr [38].

Islam [39] et al. worked on the optimized hybrid model for a stand-alone power plant in Saint martin’s island with the integration of a combination of solar PV, wind turbine, battery and diesel generator. The best combination is of a Solar PV (8kW), 2 wind turbines each having 3 kW output, diesel generator (15 kW) and 25 batteries (800 Ah each) [39]. This architecture results in lowest COE BDT 26.54 / kWh (US$ 0.345/kWh) and total net present cost (NPC) of BDT 10,620,388 (USD$ 137,927) with a renewable fraction of 31% [39].

From the literature review, it is evident that, most of the presented solutions for powering Saint Martin’s Island are simulation-based hybrid systems with inclusion of solar, wind and backup generators. The project’s capital cost, operational cost and payback periods are large in number and there are sustainability issues in terms of efficiency and lifetime of some of the system components. On the other hand, thermodynamic conversion process for generating electricity is much more efficient and sustainable technology for longer run. So, in the current work, a CSP based (Parabolic Trough Collector-PTC) off-grid power plant is designed and optimized for Saint Martin’s Island, which will solve the power problem in a sustainable and efficient way.

4. Methodology

4.1. Power Plant Architecture

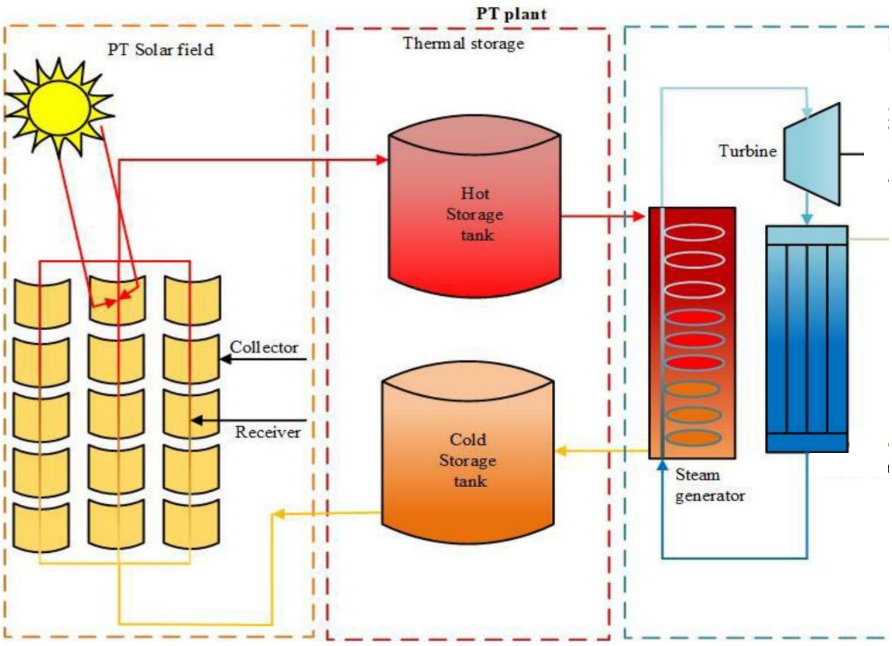

Figure 13 : Power plant architecture for the optimized design

The power plant uses CSP technology to generate power from incident solar radiation. Different units of the power plant are being described below:

4.1.1. PT Solar Field

The PT solar field consists of several numbers of parabolic trough collector along their axis flows a tube where the Heat Transfer Fluid (HTF) flows and absorbs heat reflected from the polished metal mirrors of the PTC[40].

4.1.2. Collector

Parabolic trough collector (PTC) is currently the most matured technology which is currently installed in numerous CSP plants around the world. PTC is the selected collector type for this study considering the relevant experience and relative cost. An overview of the PTC technology is presented below.

A parabolic trough is constructed by bending a reflective sheet (usually silvered acrylic) into the shape of a parabola. Several sheets are joined together to form a series of reflectors. An absorber pipe coated in black color is placed along the focal line of the collector. The solar radiation is concentrated on the absorber tube as the parabolic collectors are facing the sun. A single axis tracking mechanism is sufficient to ensure maximum exposure to the solar radiation. The black pipe is enclosed in a glass tube to minimize heat loss by convection. Although the metal tube is often coated with material with high solar absorbance characteristics, the glass tube is covered in antireflective coating to enhance transmissivity. **Figure 14** [41] illustrates the different elements of a PTC.

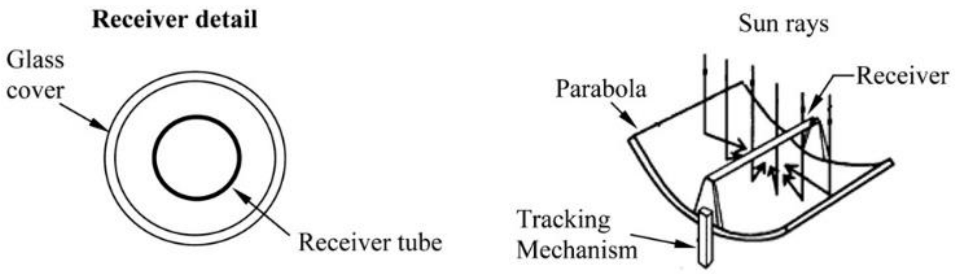

Figure 14 : Schematic of a parabolic trough collector [41]

4.1.3. Thermal Storage

The hot heat transfer fluid (HTF) flows from the PTC to the hot storage tank from which it flows to the power unit. After exchanging heat with the power unit, the cold HTF flows back to the Cold storage tank where it is being kept as the thermal storage medium for further power backup while no solar radiation present [42].

The primary selection criteria for a suitable storage media can be identified as a combination of high energy capacity and high efficiency material that ensures good heat transfer capability between the HTF and the storage medium. A. Gil [43] et al. suggested a complete list of requirements for a thermal storage system:

- Storage capacity of high energy density
- Stability in terms of mechanical and chemical properties
- Compatibility between heat transfer fluid, heat exchanger and/or storage medium to guarantee safety
- Good heat transfer between storage medium and HTF
- Low thermal losses
- Ease of control
- Operation strategy

- Maximum load imposed
- Nominal temperature selection

D. Fernandes [44] et al. presents an extensive guideline in selecting the suitable material as a TES solution for a specified case. The first step is to choose a suitable form of thermal storage. The three forms that can be found are listed as latent heat storage, sensible heat storage and thermo-chemical storage. Latent storage systems rely on phase change materials (PCMs) to store heat where the storage media undergoes a phase change while rejecting or absorbing heat. PCMs are gaining high interest to be used as HTTES for concentrating solar power applications. But PCMs possess low thermal conductivity which leads to low charging and discharging rates [45]. From the presentation [46][47] of the physical and thermodynamic properties of various PCM candidates, it is quite obvious that the characteristics of the PCMs currently under study need to be improved to meet the high melting point requirements for using them as HTTES.

The principle of thermochemical storage system is based on a reversible reaction[48]:

$$A + heat \leftrightharpoons B + C$$

A thermochemical material converts to two separate components B and C by absorbing heat. B and C can be stored separately and combined back to material A while releasing heat. The storage capacity is characterized by the heat produced during the reverse reaction. A recent study by D. Aydin [49] presented a comprehensive review of the thermochemical heat storage system (THS). THS has distinctive advantages over sensible and latent heat storages in terms of energy storage capacity and heat losses [48]. THS can avail 8 to 10 times higher energy density when compared to SHS and 2 times higher when compared to LHS. The high energy capacity is a very useful characteristic particularly for applications where space is limited and a compact storage system is an important design factor.

However, the design of THS based plants demands a high degree of efficiency in heat and mass transfer from the storage volume to ensure efficient reaction of the storage material. This may result in limiting the storage volume. Despite the continuous efforts to develop the THS technology, this concept has not yet been fully developed for commercialization.

Sensible heat storage (SHS) materials are characterized as a group of materials that do not go under phase change in the temperature range of the storage materials [44]. The energy density of a specific material influences its ability to store sensible heat. **Table 5** presents the major characteristics of common sensible heat storage materials [47][44].

Table 5: Main characteristics of sensible heat storage materials. [47]

Storage medium	Temperature Cold (℃)	Temperature Hot (℃)	Average density (kg/m³)	Average heat conductivity (W/m K)	Average heat capacity (kJ/kg K)	Volume specific heat capacity (kWh_t/m^3)	Costs per kg (US$/kg)	Costs per kWh_t ($US\$/kWh_t$)
Solid Storage Medium								
Sand-rock-mineral oil	200	300	1700	1	1.3	60	0.15	4.2
Reinforced Concrete	200	400	2200	1.5	0.85	100	0.05	1
NaCl (Solid)	200	500	2160	7	0.85	150	0.15	1.5
Cast Iron	200	400	7200	37	0.56	160	1	32
Silica fire bricks	200	700	1820	1.5	1	150	1	7
Magnesia fire bricks	200	1200	3000	1	1.15	600	2	6
Liquid storage medium								
HITEC solar salt	120	133	1990	0.60	-	-	-	-
Mineral oil	200	300	770	0.12	2.6	55	0.3	4.2
Synthetic oil	250	350	900	0.11	2.3	57	3	42
Silicon oil	300	400	900	0.1	2.1	52	5	80
Nitrite salts	250	450	1825	0.57	1.5	152	1	12
Nitrate salts	265	565	1870	0.52	1.6	250	0.5	3.7
Carbonate salts	450	850	2100	2	1.8	430	2.4	11
Liquid sodium	270	530	850	71	1.3	80	2	21

From **Table 5**, nitrate solar salt can be selected as a possible candidate as a liquid sensible heat storage medium in terms of favorable characteristics. U. Herrmann [50] et al. identifies a binary salt mixture of $NaNO_3$ and KNO_3 to be the best one in terms of cost among three nitrate salts- the other two being Hitec and HitecXL®. A mixture of 60 wt% $NaNO_3$ and 40 wt% KNO_3 is known as Solar Salt [51]. Properties of Solar Salt are presented in Table 5. High efficiency Rankine cycle turbines can be used in a Solar Salt based system due to its upper stability temperature limit $(600℃)$. Moreover, it's a non-toxic and reliable material which is available commercially. From the discussion above, Solar Salt is clearly the best candidate for a cost effective and simple design for a CSP-TES based power plant in Bangladesh that meets most of the criteria for a suitable TES media. In this configuration, Solar Salt serves as both the HTF and TES- allowing a simple design of the plant. The excess energy produced during daytime is collected in the hot storage tank to extend production after sunset.

4.1.4. Power Unit

The power unit consists a steam generator where steam is being produced by exchanging heat with HTF. The high velocity high pressure steam is then flown through the turbine in which the rotor reaction rotates the shaft of the generator producing the desired power output. Steam then flows through a condenser in which by an air cooling system the steam releases heat and changes its phase into water [52].

4.1.5 Power Cycle

The default power plant implemented in SAM uses Rankine cycle with two feedwater heaters in the configuration [53].

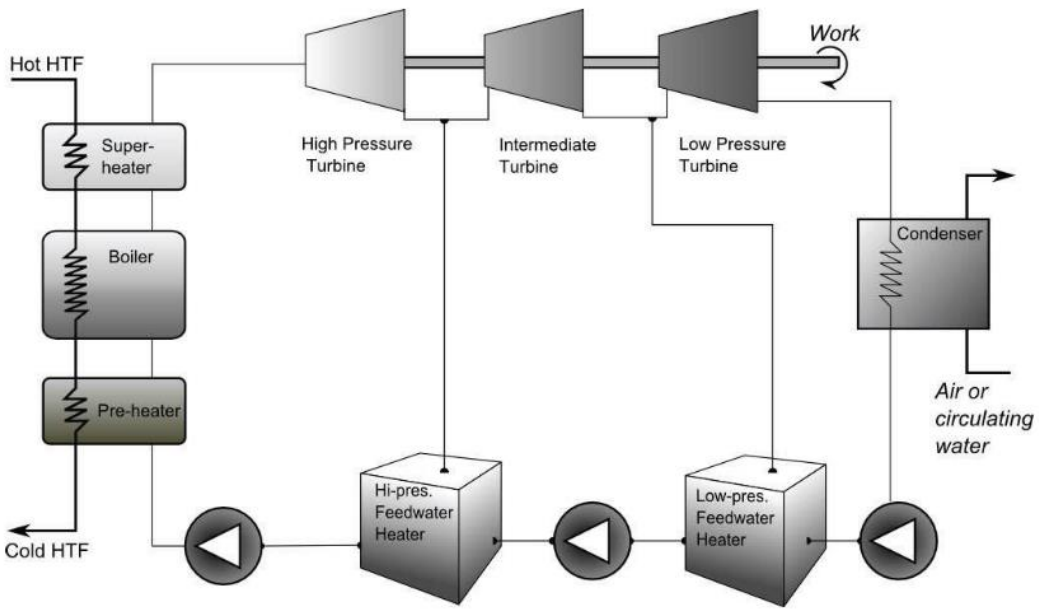

Figure 15 : Power Cycle of the system [53]

5. Modeling and Simulation

5.1. SAM Description

The System Advisor Model (SAM) is a software that is primarily used by people working in the renewable energy sectors [7]. SAM is funded by U.S. Department of Energy and developed by the National Renewable Energy Laboratory (NREL).

This software can be used to make design estimations and perform economic analyses for various technologies including photovoltaics, concentrating solar power, wind power, geothermal, biomass power etc. The main application of SAM is to make predictions based on system design parameters and installation costs to evaluate feasibility of the design under consideration.

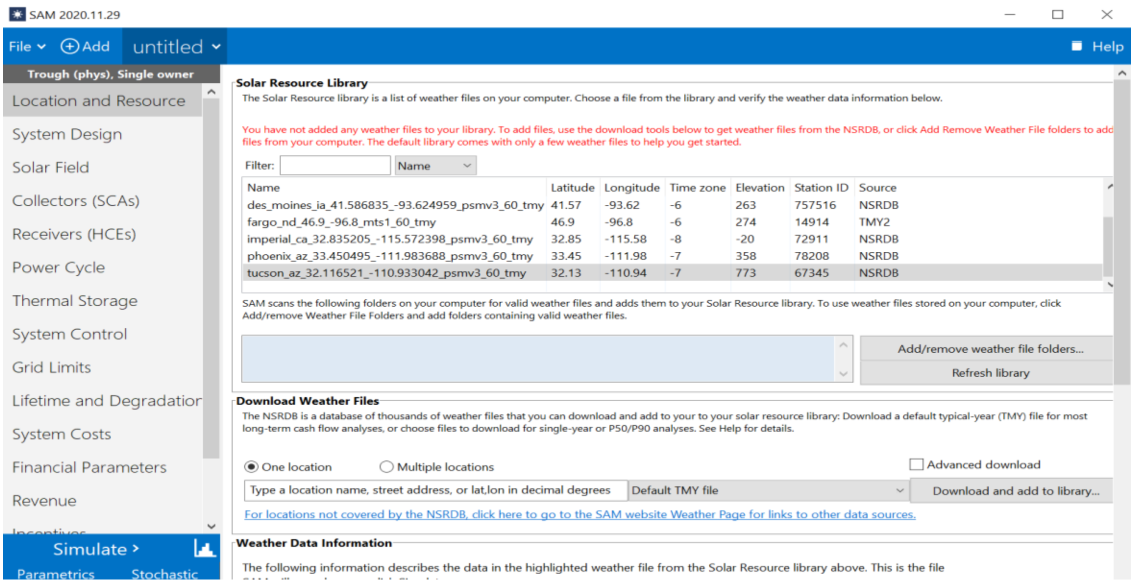

Figure 16 : SAM User Interface

The CSP model used in this study is the physical trough model in SAM. The physical model utilizes the first principles of heat transfer and thermodynamics, rather than empirical relations.

5.2. Mathematical Model

The steady-state form of the mathematical model for the PTC based power block is based on John A. Duffie [54].

Total solar power incident on parabolic trough,

$$Q_I = I_b \cdot A_a \cdot N_m \cdot N_r \cdot cos\theta \quad (1)$$

Absorber area,

$$A_a = (W - D_{co})L \quad (2)$$

Total solar power absorbed by receiver,

$$Q_a = I_b \cdot K(\theta) \cdot A_a \cdot N_r \cdot N_m \cdot r_g \cdot \gamma_r \cdot \alpha_a \cdot IF \cdot \eta_d \cdot EndLoss \quad (3)$$

Where-

$$EndLoss = 1 - \frac{f tan\theta}{L_{sc}} \quad (4)$$

Where f is the focal length of the collector and Lsc is the length of a collector which can be calculated as,

$$L_{sc} = Length\ of\ each\ module \cdot N_m \quad (5)$$

The useful power gain in a single module of the receiver is calculated as,

$$Q_{u_{module}} = F_R \left[\frac{Q_a}{N_r N_m} - A_r U_L (T_i - T_a)\right] \quad (6)$$

Where absorber area for a single module,

$$A_r = \pi \cdot D_i \cdot L \quad (7)$$

Collector heat removal factor,

$$F_R = \frac{m_f C_p f}{U_L A_r}[1 - e^{-(\frac{U_L A_r \grave{F}}{m_f C_{pf}})}] \quad (8)$$

Collector efficiency factor,

$$\grave{F} = \frac{1}{U_L\left[\frac{1}{U_L} + \frac{D_o}{D_i h_f} + \frac{D_o}{2k_r}\left(\ln\frac{D_o}{D_i}\right)\right]} \tag{9}$$

The thermodynamic properties of Solar Salt can be expressed as functions of temperature [55],

$$C_{pf} = 1443 + 0.172 \cdot T(℃) \tag{10}$$

$$\rho_f = 2090 - 0.636 \cdot T(℃) \tag{11}$$

$$\mu_f = \begin{bmatrix} 22.714 - 0.120 \cdot T(℃) + 2.281 \times 10^{-4} \cdot T^2(℃) \\ -1.474 \times 10^{-7} \cdot T^2(℃) \end{bmatrix} \times 10^{-3} \tag{12}$$

$$k_f = 0.443 + 1.9 \times 10^{-4} \cdot T(℃) \tag{13}$$

5.3. SAM Input Parameter Selection

SAM provides validated and tested default input parameters for all the models. The user is supposed to change the parameters that are directly or indirectly affected by the selection of location and design parameters. The selection method of the various parameters that are affected by our design choice is presented below.

5.3.1. System Design

Table 6: System design parameters

Parameter	Value
Solar Multiple	2
Design Point DNI	$852\ W/m^2$
Loop inlet HTF temperature	293℃
Loop outlet HTF temperature	550℃
Design turbine gross output	$1\ MWe$
Estimated gross to net conversion factor	0.9
Cycle thermal efficiency	0.4058
Hours of storage at design point	$12\ hours$

Design point DNI

This is basically the maximum field collector DNI-cosine product which has been chosen as described in SAM documents. The quantity of dumped energy might increase if the chosen DNI value is too low. On the other hand, too high of a value for reference DNI results in an undersized field. The issue with an undersized field is that it runs the power block only a few times at its design capacity throughout the year.

Loop inlet and outlet temperature

Chosen according to the operational range for Hitec Solar salt.

Design turbine gross output

This value was set by estimating the future demand after a thorough field survey.

Cycle thermal efficiency

The thermal efficiency of the molten power tower model in SAM was used as the reference value for Carnot scaling as per the design ambient temperature.

Hours of storage at design point

The power plant is expected to supply power throughout the night. So, the hours of storage have been set as 12 hours.

5.3.2. Receiver

Table 7: Receiver parameters

<table>
<tr><th>Parameter</th><th colspan="2">Value</th></tr>
<tr><td>Model</td><td colspan="2">Schott PTR 70 2008</td></tr>
<tr><td>Primarily installed units</td><td colspan="2">75%</td></tr>
<tr><td>Replacement of damaged units</td><td colspan="2">25%</td></tr>
<tr><td rowspan="3">Estimated avg heat loss</td><td>Vacuum (95%)</td><td>$317\ W/m$</td></tr>
<tr><td>Air (Lost Vaccum) (1%)</td><td>$1802\ \mathrm{W/m}$</td></tr>
<tr><td>Air (Broken Glass) (0.5%)</td><td>$4637\ \mathrm{W/m}$</td></tr>
<tr><td>Absorber material type</td><td colspan="2">304L Steel</td></tr>
<tr><td>Absorber tube inner diameter</td><td colspan="2">$0.066m$</td></tr>
<tr><td>Absorber tube outer diameter</td><td colspan="2">$0.07m$</td></tr>
<tr><td>Glass envelope inner diameter</td><td colspan="2">$0.115m$</td></tr>
<tr><td>Glass envelope outer diameter</td><td colspan="2">$0.12m$</td></tr>
<tr><td>Absorber flow plug diameter</td><td colspan="2">$0m$</td></tr>
<tr><td>Internal surface roughness</td><td colspan="2">4.5×10^{-5}</td></tr>
<tr><td>Absorber flow pattern</td><td colspan="2">Tube flow</td></tr>
</table>

The Schott PTR 70 2008 receiver model was used due to its availability and experience of being installed at several locations around the world. It was assumed that over the life of the project, 1% of the installed receivers have lost vacuum in the annulus and another 0.5% have broken glass. It was also assumed that 25% of the damaged receivers are replaced with intact units. The estimated average heat loss was found to be $353.45\ W/m$. This value is used for sizing the field only- it doesn't affect the simulated parameters. The heat loss values are obtained from a correlation used in the heat loss testing of the receiver model performed by NREL [56].

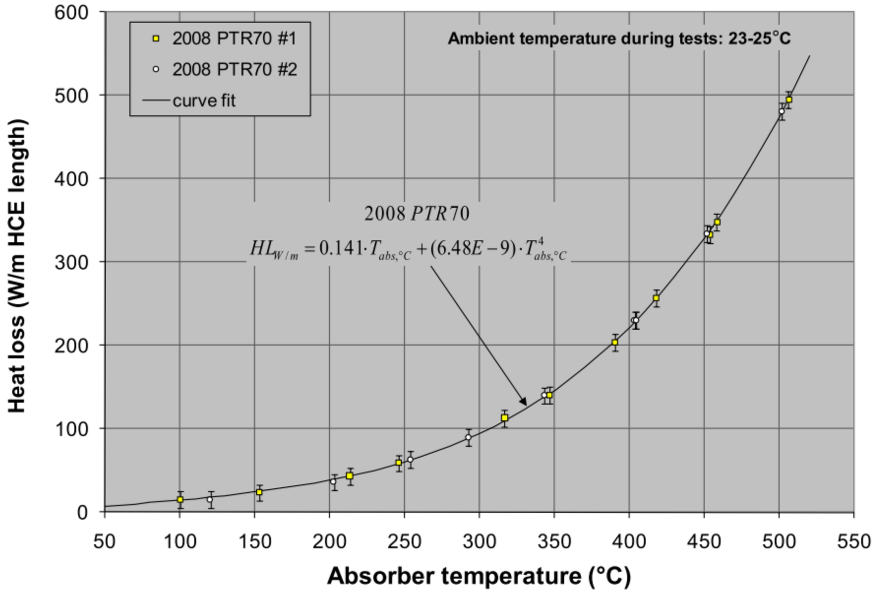

Figure 17 : 2008 PTR70 heat loss results (for intact receivers) [56]

The correlation used for calculating heat loss in SAM is presented below. It was developed by Price[57] to correlate heat loss to temperature, effect of the ambient temperature, wind speed and the rise of absorber tube temperature above the HTF temperature by the sun.

The vacuum of the HCEs in the field might be lost due to some occurrences like broken glass and presence of leak in the glass envelope. In the first case, the HCEs' glass envelope is considered to be completely missing. So, the absorber directly exchanges heat with the environment. For the second case, air is considered to have leaked through the glass envelope- altering the pressure inside the annulus from vacuum a to atmospheric pressure.

Average heat loss per unit HCE length,

$$HL_{avg} = \frac{\int_{Ti}^{To} (A0 + A1 \cdot (T_{HTF} - T_{amb}) + A2 \cdot T_{HTF}^2 + A3 \cdot T_{HTF}^3 + A4 \cdot I_b IAM \cdot cos\theta \cdot T_{HTF}^2 + \sqrt{V_w} \cdot (A5 + A6 \cdot (T_{HTF} - T\_amb))) \cdot dT_{HTF}}{(T_o - T_I)} \tag{14}$$

Which simplifies to,

$$HL_{avg} = \frac{HL_{Term1} + HL_{Term2} + HL_{Term3} + HL_{Term4}}{(T_o - T_i)} \tag{15}$$

Where-

$$HL_{Term1} = \left(A0 + A5 \cdot \sqrt{V}\right)(T_o - T_i) \tag{16}$$

$$HL_{Term2} = \left(A1 + A6 \cdot \sqrt{V_w}\right)\left(\frac{T_o^2 - T_i^2}{2} - T_{amb} \cdot (T_o - T_i)\right) \tag{17}$$

$$HL_{Term3} = \left(\frac{A2 + A4 \cdot I_b \cdot IAM \cdot cos\theta}{3}\right)(T_o^3 - T_i^3) \tag{18}$$

$$HL_{Term4} = \frac{A3}{4}(T_o^4 - T_i^4) \tag{19}$$

And

$$T_i = Inlet\ temperature\ in\ each\ loop, ℃$$

$$T_o = Oulet\ temperature\ in\ each\ loop, ℃$$

$$\theta = Incidence\ angle$$

$$Incidence\ angle\ modifier, IAM = cos\theta - 0.000884 \cdot \theta - 0.00005369 \cdot \theta^2$$

The incidence angle varies throughout the year. So, the incidence angles for the entire year were collected from the SAM weather file and fed in a MATLAB program which was used to calculate the average heat loss coefficients. The coefficients A0 through A6 were calculated using experimental data by least square curve fitting. These coefficients for different cases are presented below in Table 8.

Table 8: SAM Heat loss correlation coefficients for the 2008 PTR70 [56]

Case	Heat loss coefficient	2008 PTR70
Vacuum	A0	4.05
	A1	0.247
	A2	-0.00146
	A3	5.65E-06
	A4	7.62E-08
	A5	-1.70
	A6	0.0125
Hydrogen	A0	11.8
	A1	1.35
	A2	7.50E-04
	A3	4.07E-06
	A4	5.85E-08
	A5	-4.48
	A6	0.285
Lost vacuum	A0	50.8
	A1	0.904
	A2	5.79E-04
	A3	1.13E-05
	A4	1.73E-07
	A5	-43.2
	A6	0.524
Broken	A0	-9.95
	A1	0.465
	A2	-8.54E-04
	A3	1.85E-05
	A4	6.89E-07
	A5	24.7
	A6	3.37

Absorber Emittance

The absorber emittance values used in SAM follows the equation below:

$$\varepsilon = 0.062 + (2.00e - 7) \cdot T^2_{abs(°C)} \quad (20)$$

This equation was developed by NREL using experimental data (**Figure 18**).

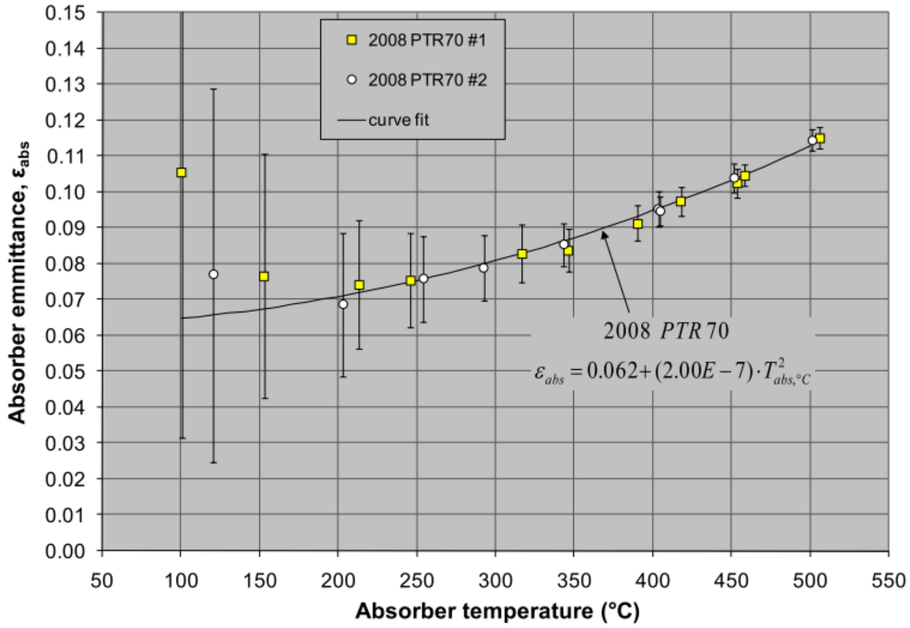

Figure 18: Absorber emittance values calculated from heat-loss testing [56]

5.3.3. Collector

The Solargenix SGX-1 collector was used with $470.3m^2$ receiver in the present model. The geometric and optical parameters are already listed in SAM library and these parameters are basically specified by the manufacturer.

The collector parameters are presented in the Table 9 given below.

Table 9: Collector parameters

Collector	
Parameter	**Value**
Model	Solargenix SGX-1
Reflective aperture area	$470.3\ m^2$
Number of modules per assembly	12
Length of collector assembly	$100\ m$
Aperture width, total structure	$5m$
Average surface-to-focus path length	$1.8m$
Piping distance between assemblies	$1m$
Incidence angle modifier coeff. F0	1
Incidence angle modifier coeff. F1	0.0506
Incidence angle modifier coeff. F2	-0.1763
Tracking error	0.988
Geometry effects	0.98
Mirror reflectance	0.935
Dirt on mirror	0.95
General optical error	0.99

5.3.4. Solar Field

Table 10: Solar field parameters

Parameter	Value	Parameter	Value
Field HTF fluid	Hitec Solar Salt	Header design min flow velocity	0.7
Design loop inlet temperature	$293℃$	Number of field subsections	2
Design loop outlet temperature	$550℃$	Freeze protection temperature	$260℃$
Max single loop flow rate	12.6	Number of SCA assemblies per loop	16
Min single loop flow rate	2.75	Actual number of loops	1
Header design max flow velocity	1.25	Total land area	8 acres
Header pipe roughness	4.57×10^{-5}	Defocusing status	Partial simultaneous defocusing
Washes per year	63	HTF pump efficiency	0.85
Water usage per wash	$0.7L/m^2$, aperture	Row spacing	$15m$

Selection of max single loop HTF flowrates and Number of SCA assemblies per loop

The pressure drop across the pipe is highly reliant on the maximum single loop flowrate. The viscosity of Hitec Solar Salt is quite higher than Therminol VP-1 which in turn causes the pressure drop to increase. The pressure building in the cold header might cause damage to the pipes if the default flowrate values are not adjusted correctly. So, it was needed to adjust both the number of SCA's and HTF flowrate to match the pressure limit of the pipe material. Instead of performing direct calculations, the default values were used to iteratively solve pipe pressure loss equations to obtain the values.

Figure 19 shows that the convergence is achieved at 15 SCAs. But as it must be an even number, so 16 SCA's was selected to be the optimum value for the present case. The maximum single loop mass flow rate is calculated to be $12.6\ kg/s$.

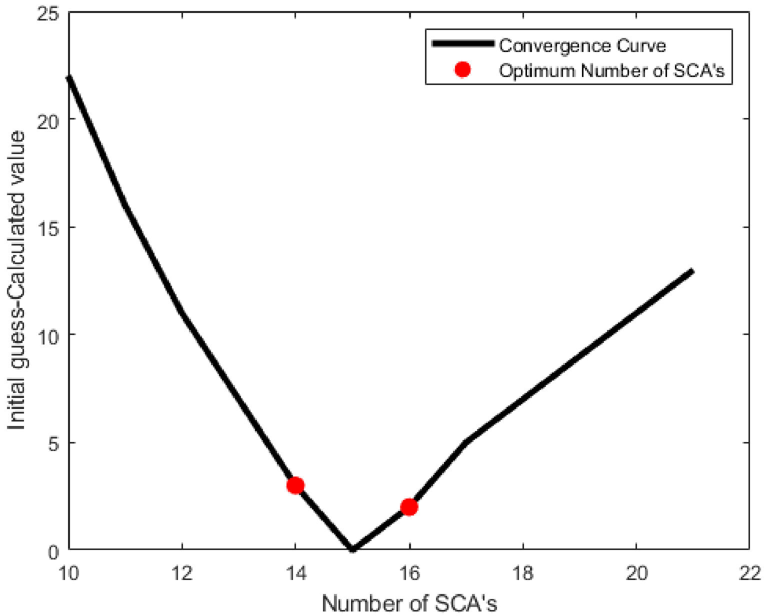

Figure 19: Selection of max single loop HTF flowrates and Number of SCA assemblies per loop.

Selection of min single loop flowrate

A parametric simulation was run to find the optimum value for the minimum single loop flowrate. **Figure 20** shows that a mass flowrate of 2.75 kg/s effectively minimizes the PPA price.

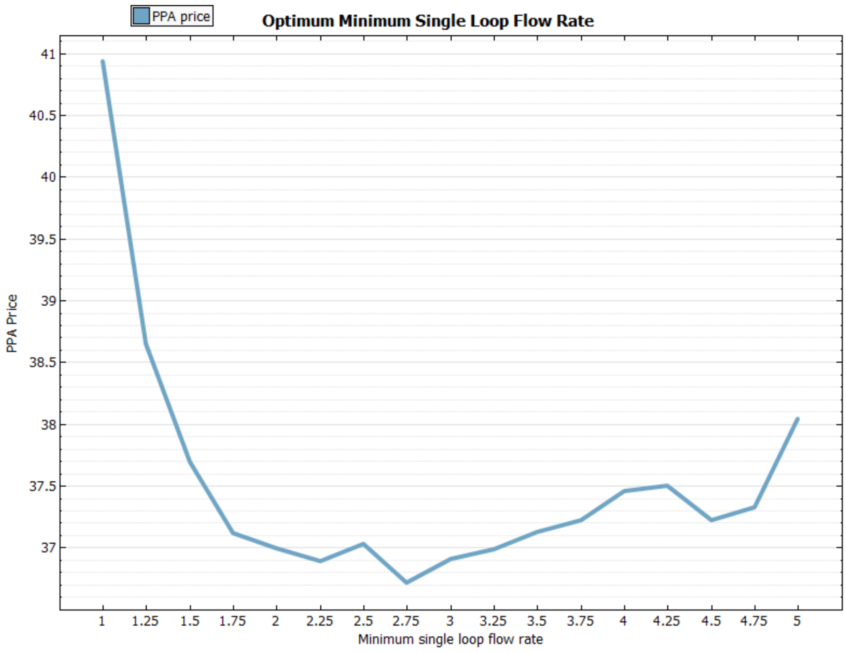

Figure 20: Optimum minimum single loop flow rate

The header design max flow velocity

Another parametric simulation was run to observe the change in header pipe pressure by varying the header design max velocity. The simulation shows that for a velocity above $1.25\ ms^{-1}$, the pressure keeps increasing beyond the allowable pressure limit (**Figure 22**). A separate parametric simulation shows that the PPA keeps increasing with decreasing velocity (**Figure 21**). So, $1.25\ ms^{-1}$ is selected as the optimum value for this parameter.

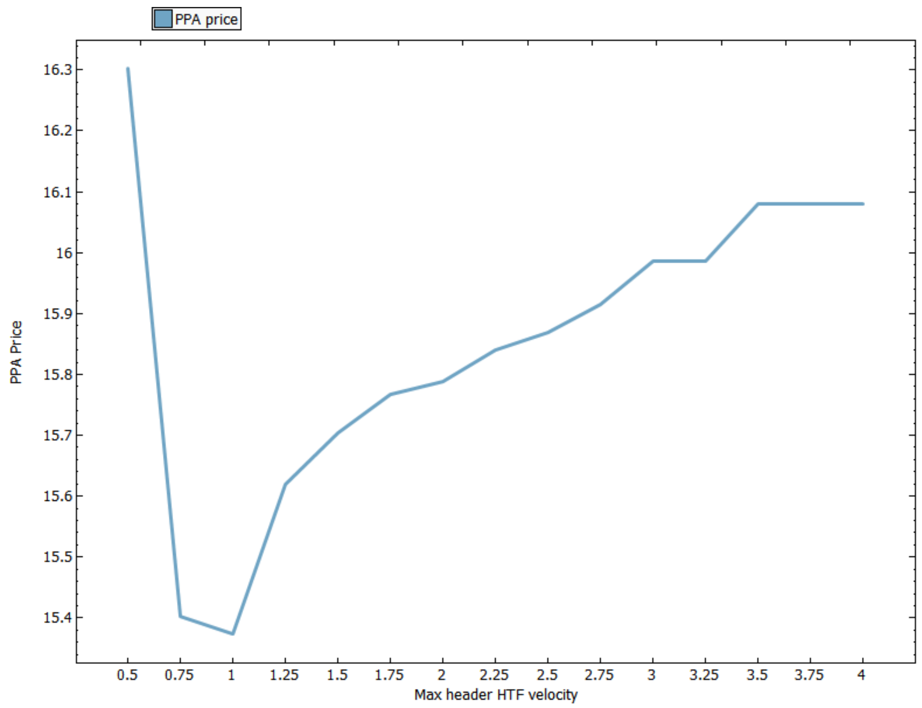

Figure 21: Variation of PPA price with Max header HTF velocity

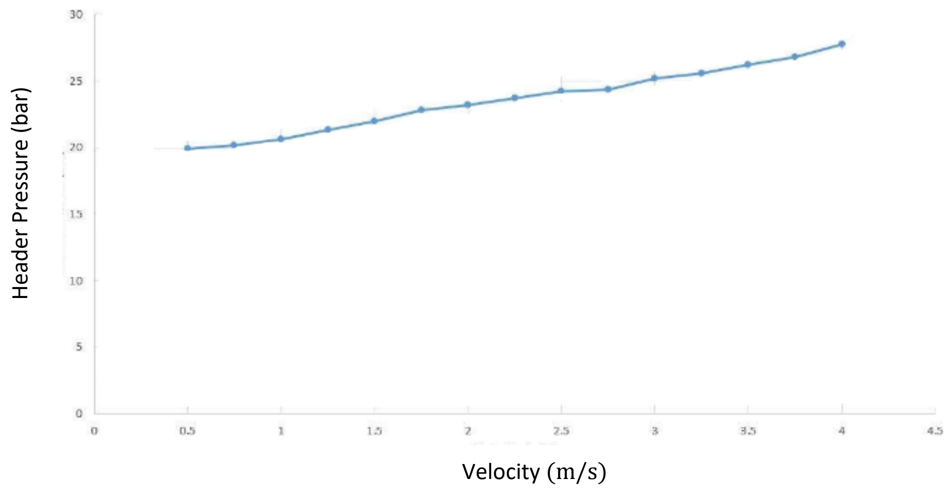

Figure 22 : Variation of Header Pressure with Velocity

Number of field subsections

The parametric simulation presented below (**Figure 23**) shows that the optimum design configuration includes 2 field subsections as it minimizes the PPA price and maximizes the Capacity factor.

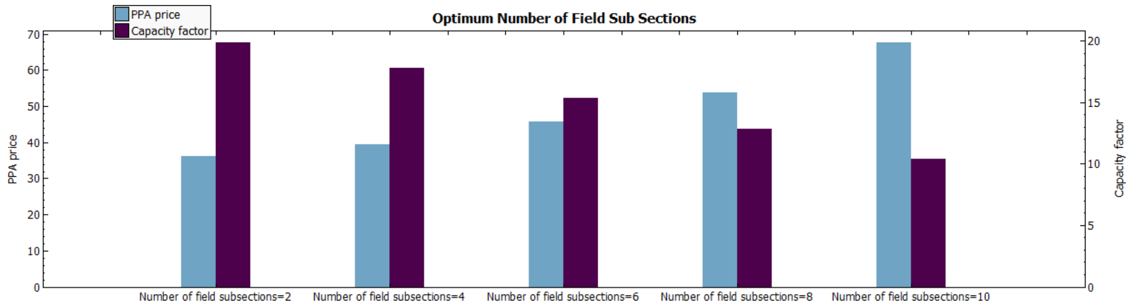

Figure 23 : Optimum number of Field Sub Sections

Defocusing Status

During hours when the collector system receives too much energy, the mass flow rate keeps increasing to maintain the design outlet temperature and eventually exceeds the maximum specified value [53]. The over-temperature condition of HTF can only be avoided by defocusing the collectors. SAM defocuses collectors in the solar field to reduce the overall thermal output. In partial defocusing allowed with simultaneous defocusing mode, the tracking angle can be changed slightly to defocus the collectors partially. All of the collectors in the field defocus by the same amount at the same time.

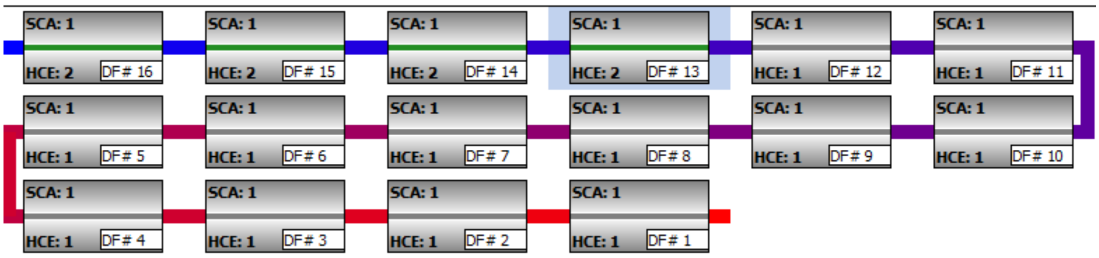

Figure 24 : Single loop configuration

Freeze Protection Temperature

Electric heating equipment's are installed in the solar field to avoid the freezing of HTF fluid. This might happen during cold weathers and long-term shutdown of the plant. Whenever there's a fall of temperature below the freeze protection temperature in any of the nodes, the heating equipment's get activated and heat is delivered to the HTF to maintain the minimum temperature. The freeze protection temperature of Hitec Solar Salt is 260℃ [50].

5.3.5. Power Cycle

The power cycle parameters are listed in the Table 11 presented below:

Table 11: Power cycle parameters

Parameter	**Value**
Boiler operating pressure	85 Bar
Condenser type	Air
Ambient temperature	36.53
Fraction of thermal power needed for standby	0.2
Power block startup time	0.5 hours
Fraction of thermal power needed for startup	0.2

The optimum boiler pressure for the Rankine cycle used in this configuration was found to be 85 bar in the literature. An air-cooled condenser was used because as shown in the **Figure 25** below, the relative humidity of Saint Martin's Island remains at a relatively higher value throughout the year. The effectivity of air-cooled and evaporative condensers relies on the dry bulb and wet bulb temperature respectively. At high relative humidity, these two temperatures become identical and so the high water-consumption associated with evaporative cooling can be avoided by using air-cooled condenser instead without any significant drop in the overall efficiency.

The power cycle used for the optimized design is regenerative Rankine cycle having two open feedwater heaters with rated cycle conversion efficiency of 40.58%. The calculative procedure for the cycle is a built-in operation within SAM.

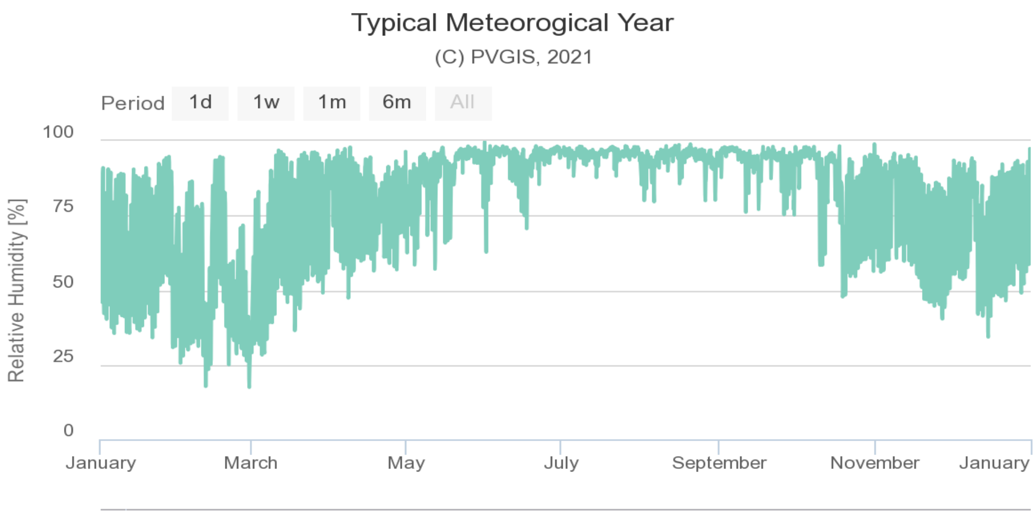

Figure 25 : Relative humidity of Saint Martin's Island throughout the year [58]

5.3.6. Thermal Storage

Thermal storage parameters are presented below in Table 12.

Table 12: Thermal storage parameters

Parameter	Value
Parallel tank pairs	2
Tank height	12 m
Cold tank heater set point	260℃
Hot tank heater set point	520℃
Storage HTF fluid	Hitec Solar Salt

Two parallel tank pairs were used to keep the tank dimensions at an optimum level considering ease of transportation, installation and maintenance. The cold and hot tank heater set points represent allowable storage fluid temperature range in the storage tanks.

6. Results and Discussions

After optimizing all the parameters, the power plant has been simulated for a year using System Adviser Model (SAM).

The Annual Gross Net Electric Output has been found to be 2,248,690 kWh and the Annual Net Electric Output is 1,161,030 kWh. The Annual Total Incident Solar Radiation has been found to be 12,220,500 kWh and the Annual Thermal Energy obtained from the solar field is 5,338,390 kWh with 5,973,280 kWh of thermal energy consumed by the power block annually. These results are shown below in **Figure 26**.

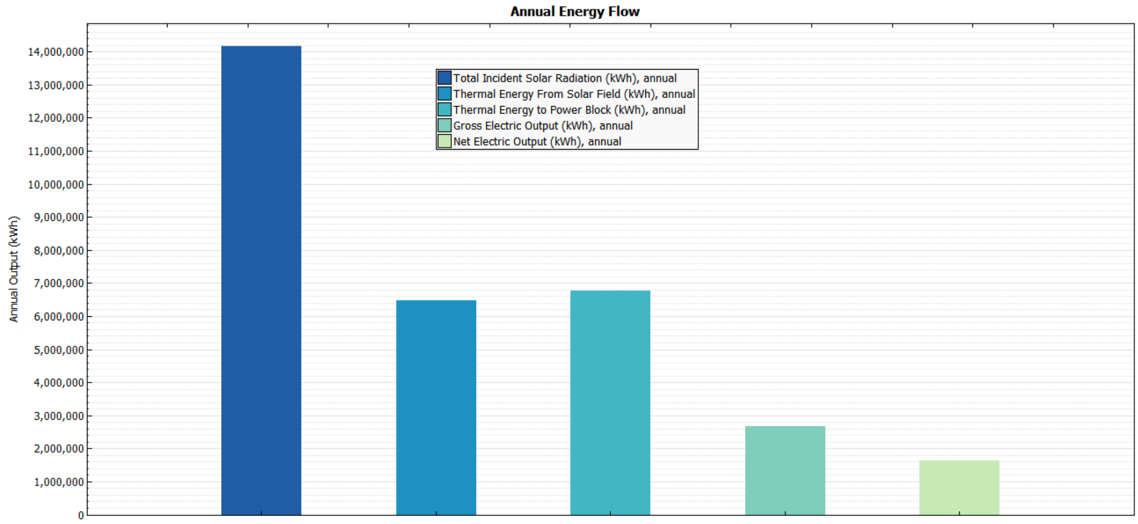

Figure 26 : Annual energy flow

Figure 27 shows that the monthly output reaches maximum (176.9 MWh) on April and minimum on July (16 MWh). The DNI remains at a lower level during the months of June, July and August (**Figure 28**) and causes the monthly output to drop at a significant level.

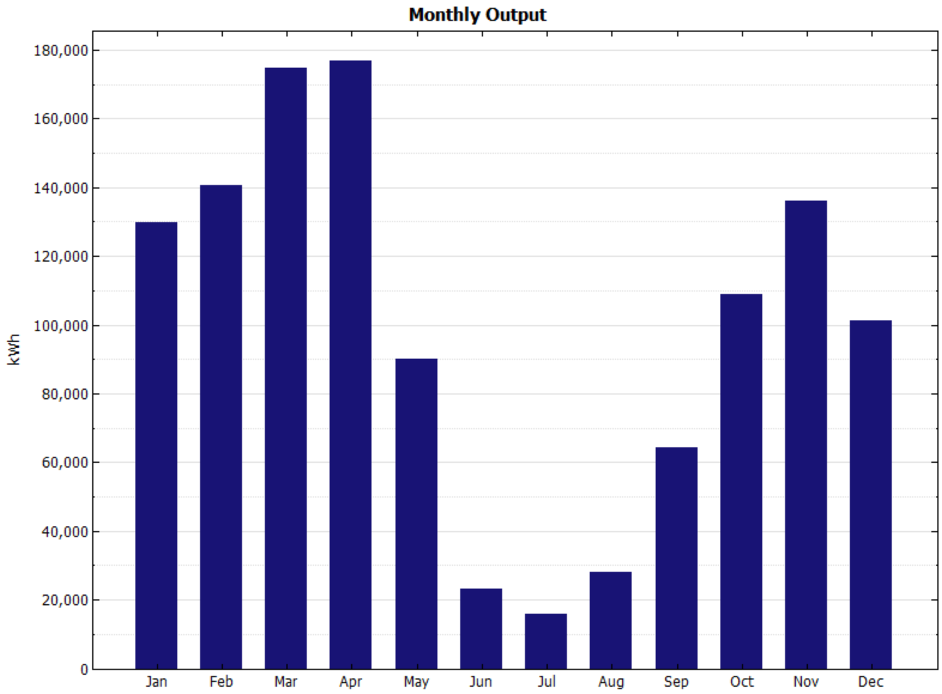

Figure 27 : Monthly output of the designed PTC power plant in St. Martins Island

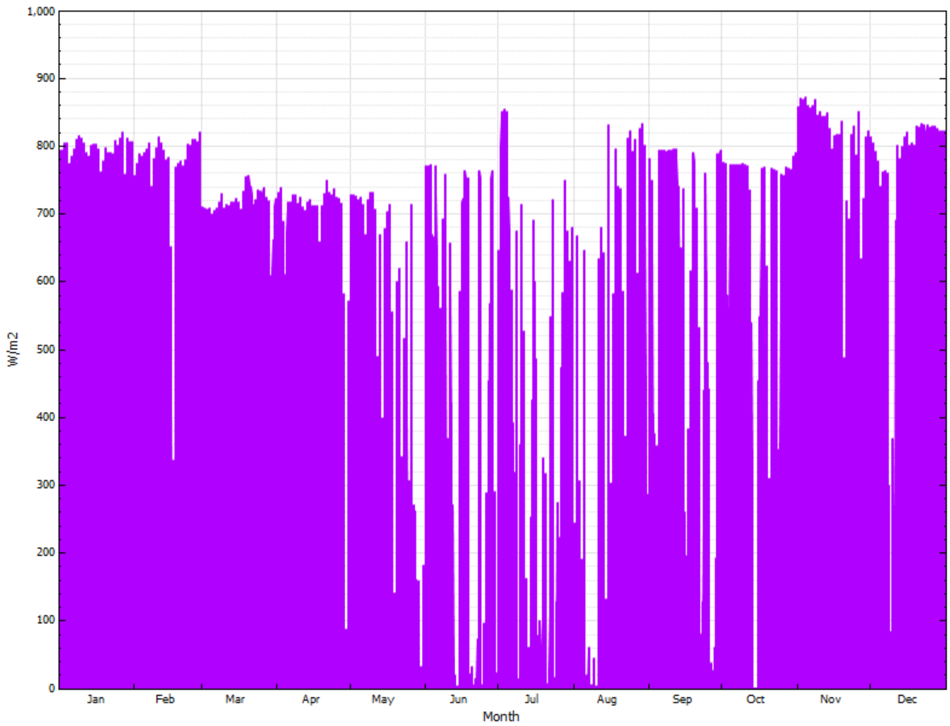

Figure 28 : Time series DNI variation

From **Figure 29**, it is seen that the First Year TOD Energy and Revenue was maximum during the month of April with obtained energy of 230,000 kWh and revenue of $ 87,000 respectively. The minimum First Year TOD Energy and

Revenue was during the month of July with obtained energy of 28,000 kWh and revenue of $ 26,000 respectively.

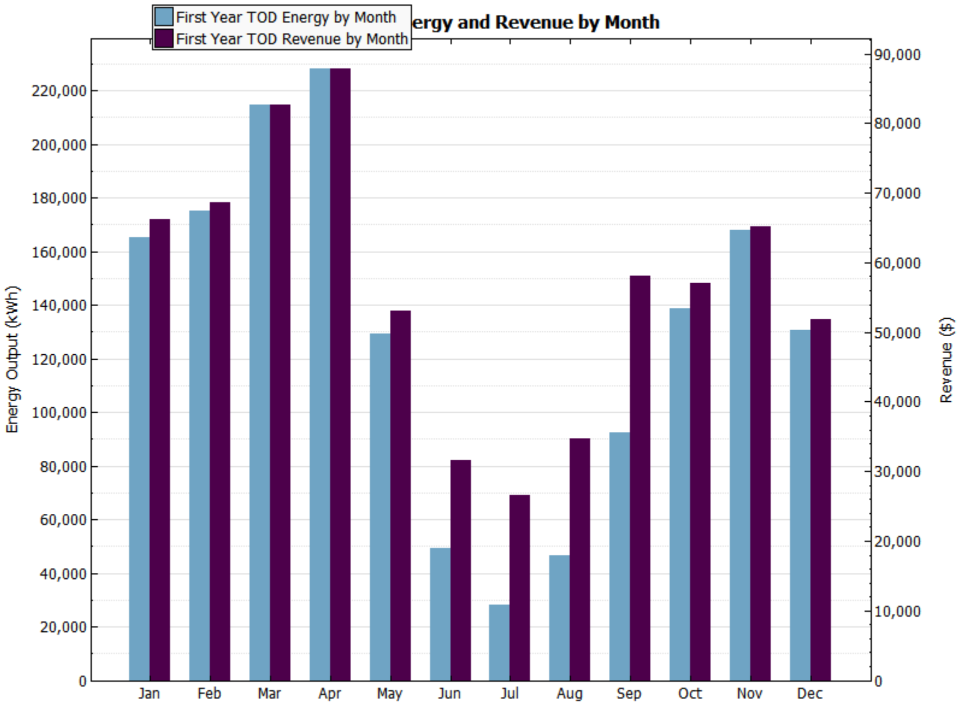

Figure 29 : First year TOD energy and revenue by month

:

Figure 30 shows that the Total Incident Thermal Energy was maximum during the month of January and minimum during the month of July with values of 1620 MWh and 540 MWh. During the month of April, the Thermal Energy Absorbed by the HTF was maximum and it was minimum during the month of July with values of 780 MWh and 280 MWh respectively.

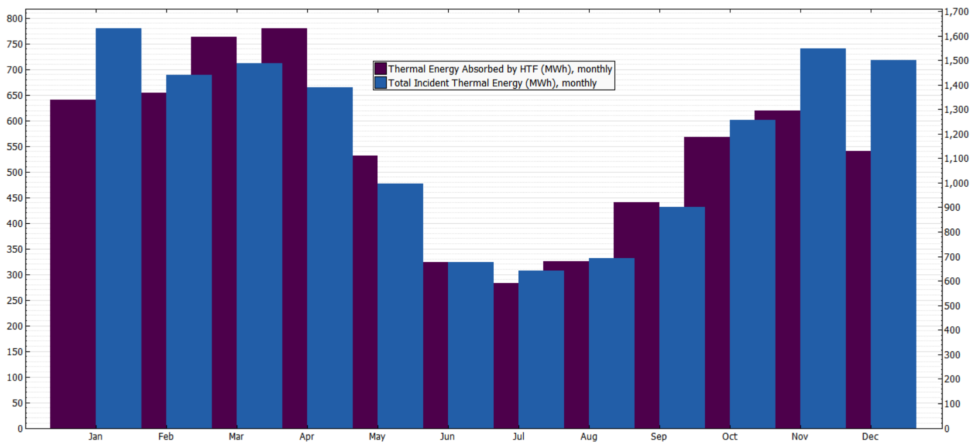

Figure 30 : Monthly incident and absorber thermal energy by HTF

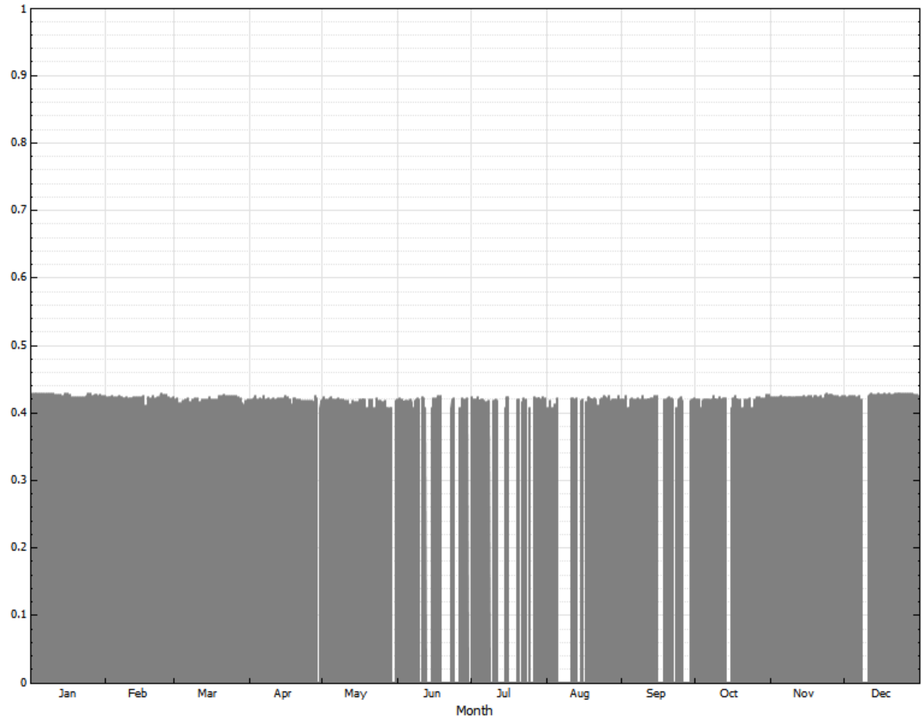

Figure 31 : Efficiency of the power cycle

The power cycle efficiency remains fairly constant at a level of around 0.41% throughout the year (**Figure 31**). During the months of June, July and August the efficiency seems to drop at zero. The reason behind this can be explained by the possibility of bad weather conditions during these months. The power generation system can be backed up for up to 12 hours. But the thermal storage system eventually runs out of energy when the sunlight is absent for an extended period of time. This might happen during the rainy season or instances of natural calamities.

The number of SCA assemblies per loop and the mass flow rate of HTF was adjusted to match the pressure drop across the solar field. The aim was to keep the pressure drop below the limit specified by the choice of absorber pipe material. **Figure 32** shows that the pressure drop clearly remains below 22 MPa which is the operational limit for steel 304L.

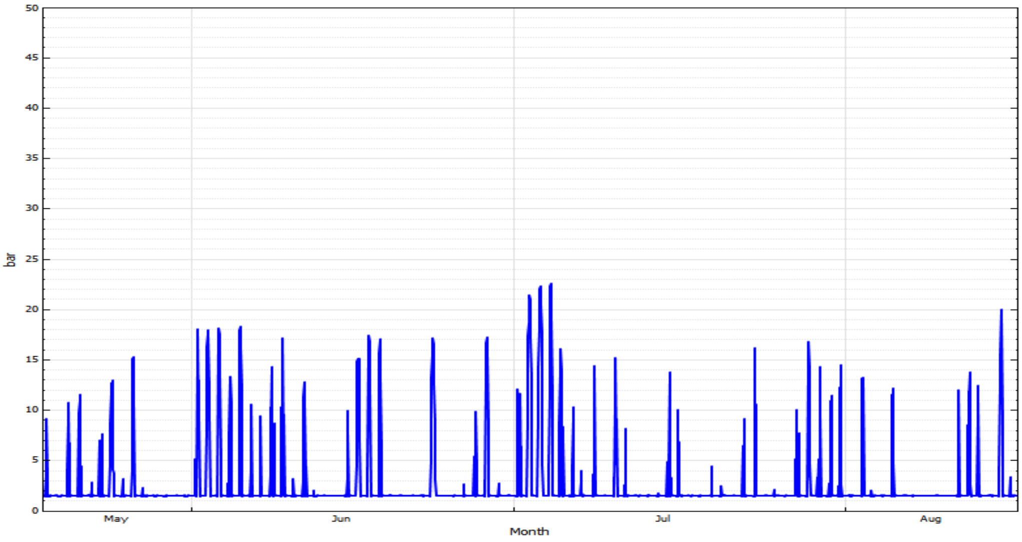

Figure 32 : Solar field pressure drop

Figure 33 presents the total receiver thermal loss (MWh) in every month and the average receiver thermal loss (W/m). The average receiver thermal loss values closely align with the estimated value (353.45 W/m). The estimated value affects the sizing of the field. Thus, our choice of the field sizing estimation has reasonable accuracy.

Figure 33 : Variation of receiver thermal loss and average receiver thermal loss.

Temperature at the hot header outlet only varies from the design outlet temperature during hours when the sunlight might be absent for prolonged periods (**Figure 34**). The temperature into and inside the hot tank remains well below the stability range of Hitec Solar Salt.

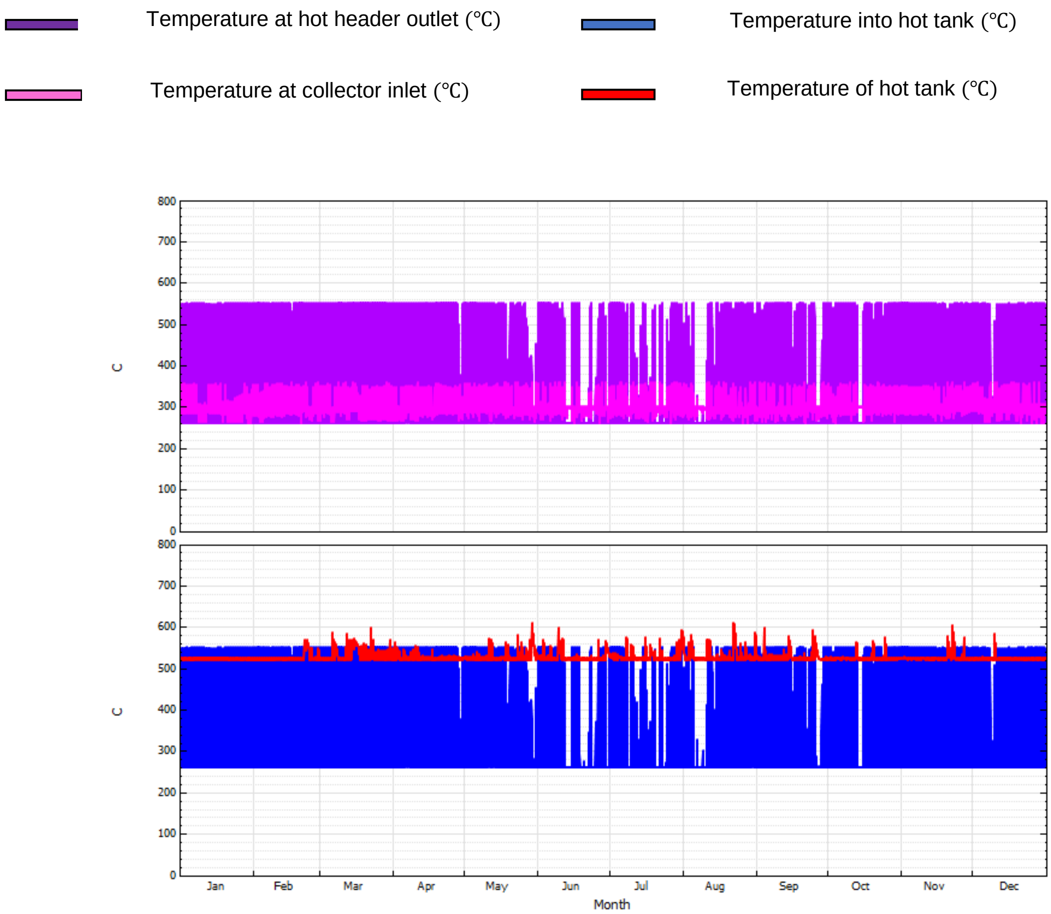

Figure 34 : Temperature at significant locations of the plant design.

The result summary of the simulation is presented in **Table 13**. The power plant has a nameplate capacity of 1 MW with a power cycle efficiency of 0.4058 and a total land area of 7.83 acres is needed, with an annual water usage of 572 m^3. The capacity factor of the plant is 19.9% with a gross to net conversion factor of 0.61.

Table 13: Result summary

Annual Energy	1.115 GWh
Nameplate Capacity	1 MW
`Capacity Factor	14.1%
Gross to net Conversion Factor	0.52
Annual Water Usage	491 m^3
Total Land Area	7.81 acre
Power Cycle Efficiency	0.4058
Power Cycle Gross Output	2.68 GWh

The plant has been designed to handle future demands keeping in mind the growing number of local inhabitants and tourists. The present model effectively minimizes the land requirement and water usage. It also ensures an uninterrupted power supply throughout the day and night as it incorporates direct thermal storage in the design. So, the present design solution may be regarded as a sustainable solution in terms of the longevity and efficiency.

Further study can be carried out to find the environmental effects. Although the solution is using renewable source of energy, but the conversion process may use other forms whose impact on the environment of this coral island is very important. This will be continued in future works.

7. Conclusion

A standalone power plant has been designed to facilitate the energy demand of the locals and tourists of the Saint Martin's island. The design capacity of the powerplant is 1MW which is sufficient to meet the present and near future energy demand of the island. The analysis shows that, the air-cooled condenser-based system is the most effective choice in terms of water consumption and revenue. Thermal storage of the plant is capable enough to supply power backup for 12 hours which is one of the key problems to be resolved in this distinct and isolated island. Only 1.08% land area of the total island is being used for this powerplant which will not impose any significant burden on the limited land area of this island. Reduction of carbon dioxide (CO_2) and carbon monoxide (CO) emission in the coral island is one of the key factors behind choosing a renewable source for power production using Parabolic trough collector (PTC) based CSP technology. The other environmental benefits that may help the coral island to sustain may be studied in future. Overall, an implementation of this type of power plant may bring huge success and explore deeply the potential in harnessing solar power through CSP technologies in Bangladesh.

8. References

[1] “https://www.iea.org/reports/world-energy-outlook-2020.” .

[2] “http://www.renewableenergy.gov.bd/index.php?id=1&i=1.” .

[3] M. M. Rhaman, “Hybrid renewable energy system for sustainable future of bangladesh,” Int. J. Renew. Energy Res., vol. 3, no. 4, pp. 777–780, 2013, doi: 10.20508/ijrer.20029.

[4] N. Bhuiyan, W. Ullah, R. Islam, T. Ahmed, and N. Mohammad, “Performance optimisation of parabolic trough solar thermal power plants–a case study in Bangladesh,” Int. J. Sustain. Energy, vol. 39, no. 2, pp. 113–131, 2020, doi: 10.1080/14786451.2019.1649263.

[5] “https://latitude.to/articles-by-country/bd/bangladesh/10284/st-martins-island.” .

[6] M. Kamruzzaman, “Assessment of Destination-specific factors of Bangladesh: A review of Saint Martin Island as an emerging Tourist Destination,” J. Bus. Stud., vol. XXXIX, no. 1, 2018.

[7] “https://sam.nrel.gov/about-sam.html.” .

[8] J. J. Burkhardt, G. A. Heath, and C. S. Turchi, “Life cycle assessment of a parabolic trough concentrating solar power plant and the impacts of key design alternatives,” Environ. Sci. Technol., vol. 45, no. 6, pp. 2457–2464, 2011, doi: 10.1021/es1033266.

[9] H. Olia, M. Torabi, M. Bahiraei, M. H. Ahmadi, M. Goodarzi, and M. R. Safaei, “Application of nanofluids in thermal performance enhancement of parabolic trough solar collector: State-of-the-art,” Appl. Sci., vol. 9, no. 3, 2019, doi: 10.3390/app9030463.

[10] H. Schenk, T. Hirsch, J. F. Feldhoff, and M. Wittmann, “Energetic comparison of linear Fresnel and parabolic trough collector systems,” J. Sol. Energy Eng. Trans. ASME, vol. 136, no. 4, pp. 1–11, 2014, doi: 10.1115/1.4027766.

[11] G. Morin, M. Karl, M. Mertins, and M. Selig, “Molten Salt as a Heat Transfer Fluid in a Linear Fresnel Collector - Commercial Application Backed by Demonstration,” Energy Procedia, vol. 69, pp. 689–698, 2015, doi:

10.1016/j.egypro.2015.03.079.

[12] W. M. Conlon, P. Johnson, and R. Hanson, "Superheated steam from CLFR solar steam generators," in American Society of Mechanical Engineers, Power Division (Publication) POWER, Feb. 2011, vol. 1, no. 1, pp. 301–307, doi: 10.1115/POWER2011-55174.

[13] T. Hirsch and A. Khenissi, "A systematic comparison on power block efficiencies for CSP plants with direct steam generation," Energy Procedia, vol. 49, pp. 1165–1176, 2014, doi: 10.1016/j.egypro.2014.03.126.

[14] C. Ortiz, M. Binotti, M. C. Romano, J. M. Valverde, and R. Chacartegui, "Off-design model of concentrating solar power plant with thermochemical energy storage based on calcium-looping," AIP Conf. Proc., vol. 2126, no. July, 2019, doi: 10.1063/1.5117755.

[15] S. Relloso and E. García, "Tower Technology Cost Reduction Approach after Gemasolar Experience," Energy Procedia, vol. 69, pp. 1660–1666, 2015, doi: 10.1016/j.egypro.2015.03.125.

[16] Https://www.energy.gov/eere/solar/downloads/concentrating-solar-power-tower-plant-illustration, "No Title." .

[17] Estela and A. T. Kearney, "Solar Thermal Electricity 2025," Clean Electr. *Demand Atractive STE Cost …*, no. June, p. 52, 2010, [Online]. Available: estelasolar.eu/Publications.

[18] O. (2005) Pitz-Paal, Robert and Dersch, Jürgen and Milow, Barbara and Téllez, Felix and Ferriere, Alain and Langnickel, Ulrich and Steinfeld, Aldo and Karni, Jacob and Zarza, Eduardo and Popel, "https://elib.dlr.de/46994/."

[19] Estela and A. T. Kearney, "Solar Thermal Electricity 2025," Clean Electr. *Demand Atractive STE Cost …*, no. June, p. 52, 2010.

[20] "https://webstore.iea.org/energy-technology-perspectives-2012."

[21] N. Noor and S. Muneer, "Concentrating Solar Power (CSP) and its prospect in Bangladesh," Proc. 1st Int. Conf. Dev. Renew. Energy Technol. ICDRET 2009, pp. 69–73, 2009, doi: 10.1109/icdret.2009.5454207.

[22] "https://pmo.gov.bd/pmolib/legalms/pdf/2009-renewable-%20energy-policy.pdf." .

[23] "First 100 kW mini grid solar PV of Bangladesh." [Online]. Available: http://energysystemsbd.com/portfolio.html#100kw_minigrid.

[24] "IDCOL Renewable Energy projects." [Online]. Available: http://www.idcol.org/old/documentation.php.

[25] K. A. Khan and S. R. Rasel, "Prospects of renewable energy with respect to energy reserve in Bangladesh," Publ. J. IJARII, no. 5, pp. 280–289, 2018, [Online]. Available: https://www.academia.edu/download/57482260/Prospects_of_Renewable_Energy_with_Respect_to_Energy_Reserve_in_Bangladesh_ijariie9090.pdf.

[26] S. Mistry, Prospect of solar energy use in bangladesh. 2009.

[27] K. A. Khan, M. S. Hossain, M. M. Kamal, and ..., "Pathor Kuchi leaf: importance in power production," Ijariie-Issn (O)-*2395 …*, no. September 2020, 2018, [Online]. Available: http://www.academia.edu/download/57589381/Pathor_Kuchi_Leaf_Importance_in_Power_Production.pdf.

[28] K. A. Khan et al., "Renewable energy scenario in Bangladesh," Ijarii, vol. 4, no. 5, pp. 270–279, 2018.

[29] A. D. D. Mahmud, "Prospects of Solar Energy in Bangladesh," IOSR J. Electr. Electron. Eng., vol. 4, no. 5, pp. 46–57, 2013, doi: 10.9790/1676-0454657.

[30] M. M. Karim, M. Anis-Uz-Zaman, A. T. Noman, H. Rashid, M. Z. Al Imran, and K. A. Al Mamun, "Feasibility Analysis and a Proposal for 1.3 MW Hybrid Renewable Power Plant for Saint-Martins Island Using HOMER," 2nd Int. Conf. Electr. Comput. Commun. Eng. ECCE 2019, pp. 1–6, 2019, doi: 10.1109/ECACE.2019.8679390.

[31] K. Foysal Haque, N. Saqib, and M. S. Rahman, "An optimized stand-alone green hybrid grid system for an offshore Island, Saint Martin, Bangladesh," Int. Conf. Energy Power Eng. Power Progress, ICEPE 2019, pp. 1–5, 2019, doi: 10.1109/CEPE.2019.8726596.

[32] M. A. H. Mondal and M. Denich, "Assessment of renewable energy resources potential for electricity generation in Bangladesh," Renew. Sustain. Energy Rev., vol. 14, no. 8, pp. 2401–2413, 2010, doi: 10.1016/j.rser.2010.05.006.

[33] "T. Khadem, S. M. B. Billah, S. Barua and M. S. Hossain, 'HOMER based hydrogen fuel cell system design for irrigation in Bangladesh,' 2017 4th International Conference on Advances in Electrical Engineering (ICAEE), Dhaka, Bangladesh, 2017, pp. 445-449, doi."

[34] S. Roy and M. M. Rhaman, "Hybrid Solar Power Plant in Saint Martin's Island can Enlarge Tourist Attraction in Bangladesh," I.J. Eng. Manuf., vol. 3, no. May, pp. 12–22, 2016, doi: 10.5815/ijem.2016.03.02.

[35] E. E. Feasibility and I. Costs, "Cost Analysis for Pollution Prevention," no. 95, pp. 1–6, 2005.

[36] "Mahmud Abdul Matin Bhuiyan, Anik Deb and Arefin Nasir. Article: Optimum Planning of Hybrid Energy System using HOMER for Rural Electrification. International Journal of Computer Applications 66(13):45-52, March 2013. Full text available. BibTeX."

[37] U. S. Mousumi, A. Zardar, and K. Z. Islam, "Techno-Economic Evaluation of Hybrid Supply System for Sustainable Powering the Saint Martin Island in Bangladesh," vol. 1, no. 1, 2020.

[38] M. B. M. Fardun, K. S. I. Sunny, and M. D. A. Satter, "Modelling and Optimization of Hybrid Power System at Coastal Area," 2nd Int. Conf. Electr. Comput. Commun. Eng. ECCE 2019, pp. 1–6, 2019, doi: 10.1109/ECACE.2019.8679410.

[39] A. K. M. Sadrul Islam, M. M. Rahman, M. A. H. Mondal, and F. Alam, "Hybrid energy system for St. Martin island, Bangladesh: An optimized model," Procedia Eng., vol. 49, no. March 2014, pp. 179–188, 2012, doi: 10.1016/j.proeng.2012.10.126.

[40] 2019 Goleman et al., "Design of Solar Field and Performance Estimation of Solar Tower Plants," J. Chem. Inf. Model., vol. 53, no. 9, pp. 1689–1699, 2019.

[41] S. A. Kalogirou, "A detailed thermal model of a parabolic trough collector

receiver," Energy, vol. 48, no. 1, pp. 298–306, 2012, doi: 10.1016/j.energy.2012.06.023.

[42] M. Chaanaoui, S. Vaudreuil, and T. Bounahmidi, "Benchmark of Concentrating Solar Power Plants: Historical, Current and Future Technical and Economic Development," Procedia Comput. Sci., vol. 83, no. Seit, pp. 782–789, 2016, doi: 10.1016/j.procs.2016.04.167.

[43] A. Gil et al., "State of the art on high temperature thermal energy storage for power generation. Part 1-Concepts, materials and modellization," Renew. Sustain. Energy Rev., vol. 14, no. 1, pp. 31–55, 2010, doi: 10.1016/j.rser.2009.07.035.

[44] A. I. Fernandez, M. Martnez, M. Segarra, I. Martorell, and L. F. Cabeza, "Selection of materials with potential in sensible thermal energy storage," Sol. Energy Mater. Sol. Cells, vol. 94, no. 10, pp. 1723–1729, 2010, doi: 10.1016/j.solmat.2010.05.035.

[45] D. Barlev, R. Vidu, and P. Stroeve, "Innovation in concentrated solar power," Sol. Energy Mater. Sol. Cells, vol. 95, no. 10, pp. 2703–2725, 2011, doi: 10.1016/j.solmat.2011.05.020.

[46] D. Fernandes, F. Pitié, G. Cáceres, and J. Baeyens, "Thermal energy storage: 'How previous findings determine current research priorities,'" Energy, vol. 39, no. 1, pp. 246–257, 2012, doi: 10.1016/j.energy.2012.01.024.

[47] N. Nallusamy, S. Sampath, and R. Velraj, "Experimental investigation on a combined sensible and latent heat storage system integrated with constant/varying (solar) heat sources," Renew. Energy, vol. 32, no. 7, pp. 1206–1227, 2007, doi: 10.1016/j.renene.2006.04.015.

[48] A. H. Abedin, "A Critical Review of Thermochemical Energy Storage Systems," Open Renew. Energy J., vol. 4, no. 1, pp. 42–46, 2011, doi: 10.2174/1876387101004010042.

[49] D. Aydin, S. P. Casey, and S. Riffat, "The latest advancements on thermochemical heat storage systems," Renew. Sustain. Energy Rev., vol. 41, pp. 356–367, 2015, doi: 10.1016/j.rser.2014.08.054.

[50] U. Herrmann, B. Kelly, and H. Price, “Two-tank molten salt storage for parabolic trough solar power plants,” Energy, vol. 29, no. 5–6, pp. 883–893, 2004, doi: 10.1016/S0360-5442(03)00193-2.

[51] R. I. Dunn, P. J. Hearps, and M. N. Wright, “Molten-salt power towers: Newly commercial concentrating solar storage,” Proc. IEEE, vol. 100, no. 2, pp. 504–515, 2012, doi: 10.1109/JPROC.2011.2163739.

[52] V. Christensen, “Ecopath with Ecosim: linking fi sheries and ecology 1 Why ecosystem modeling in fi sheries?,” WIT Trans. State Art Sci. Eng., vol. 34, pp. 1755–8336, 2009, doi: 10.2495/978-1-84564.

[53] M. J. Wagner and P. Gilman, “Technical manual for the SAM physical trough model, by National Renewable Energy Laboratory (NREL, U.S. Department of Energy),” Natl. Renew. Energy Lab., vol. 303, no. June, pp. 275–3000, 2011, [Online]. Available: http://www.nrel.gov/docs/fy11osti/51825.pdf.

[54] J. A. Duffie (Deceased), W. A. Beckman, and N. Blair, Solar Engineering of Thermal Processes, Photovoltaics and Wind. 2020.

[55] “http://helioscsp.com/sqms-concentrated-solar-power-csp-thermo-solar-salts/.”

[56] F. Burkholder and C. F. Kutscher, “Heat loss testing of Schott’s 2008 PTR70 parabolic trough receiver,” NREL Tech. Rep., no. May, p. 58, 2009, [Online]. Available: http://www.nrel.gov/docs/fy09osti/45633.pdf.

[57] H. Price, “A Parabolic Trough Solar Power Plant Simulation Model Preprint, NREL/CP-550-33209,” ISES 2003 Int. Sol. Energy Conf., no. January, 2003.

[58] Https://re.jrc.ec.europa.eu/pvg_tools/en/tools.html#TMY, “No Title.”